





## RESEARCH ARTICLE

10.1029/2021GC010042

# A Single Dras-Kohistan-Ladakh Arc Revealed by Volcaniclastic Records

Goran Andjić<sup>1,2</sup> , Renjie Zhou<sup>1</sup> , Tara N. Jonell<sup>1,3</sup> , and Jonathan C. Aitchison<sup>1</sup> 

<sup>1</sup>School of Earth and Environmental Sciences, The University of Queensland, St Lucia, QLD, Australia, <sup>2</sup>Department of Earth Sciences, Utrecht University, Utrecht, The Netherlands, <sup>3</sup>School of Geographical and Earth Sciences, University of Glasgow, Glasgow, UK

### Key Points:

- Dissimilar ages and compositions of volcaniclastic units in the Indus Suture Zone reveal arc evolution from primitive to mature stages
- Detrital zircon U-Pb ages and geochemistry, and whole-rock geochemistry support a common origin of the Dras and Kohistan-Ladakh arcs
- The recognition of a single Dras-Kohistan-Ladakh arc represents a key constraint in models of India-Eurasia convergence

### Supporting Information:

Supporting Information may be found in the online version of this article.

### Correspondence to:

G. Andjić,  
[g.andjic@uu.nl](mailto:g.andjic@uu.nl)

### Citation:

Andjić, G., Zhou, R., Jonell, T. N., & Aitchison, J. C. (2022). A single Dras-Kohistan-Ladakh arc revealed by volcaniclastic records. *Geochemistry, Geophysics, Geosystems*, 23, e2021GC010042. <https://doi.org/10.1029/2021GC010042>

Received 15 JUL 2021  
Accepted 28 FEB 2022

**Abstract** Tectonic interpretations of arc remnants in the Himalayan orogen remain uncertain, despite their important implications for the overall convergence history between India and Eurasia. Provenance results from deep-water volcaniclastic rocks of the Indus Suture Zone in Ladakh provide new constraints on the Mesozoic tectonic evolution of the Dras and Kohistan-Ladakh arcs. Detrital zircon (DZ) U-Pb ages and whole-rock geochemistry of the fault-bounded Upper Cretaceous Nindam and Paleocene Jurutze formations present age patterns and compositions that are consistent with those of the Dras and Kohistan-Ladakh arcs, respectively. The combination of DZs of the Nindam and Jurutze formations with the igneous zircons of the Dras and Kohistan-Ladakh arcs shows similar age distributions that support a Late Jurassic to Paleocene tectonic connection between all these units. We argue that the secular trends in geochemical composition of DZs and volcaniclastic material are consistent with the magmatic evolution of one convergent margin, which shifted from a primitive to a mature stage during the Late Cretaceous. The recognition of a single Dras-Kohistan-Ladakh arc sets the stage for reevaluating competing scenarios of the Mesozoic evolution of the India-Eurasia convergent system. We find that the most likely scenario is that of a Jurassic arc formed above a south-dipping intraoceanic subduction zone and accreted to Eurasia during the Early Cretaceous, after which it evolved above a north-dipping subduction zone.

**Plain Language Summary** The Himalayan orogen is the result of the collision between India and Eurasia and the closure of the intervening Neotethys Ocean. The suture zone between India and Eurasia hosts an incomplete and complex archive of the paleogeography that once existed between them prior to continent-continent collision. Investigating suture zone rocks may therefore provide valuable information on the building blocks of the orogen and the overall history of the India-Eurasia convergent system. Disparate remnants exposed in the Indus Suture Zone (Western Himalaya) suggest that volcanic arcs and sedimentary basins were formed above intraoceanic subduction zones, but there is no consensus on their original paleogeography. We discuss new and existing geological data from volcaniclastic rocks related to the Dras and Kohistan-Ladakh arcs. Our data support the existence of a single Dras-Kohistan-Ladakh arc during the Mesozoic and provide additional insights into the complexity of the pre-collisional convergence between India and Eurasia.

## 1. Introduction

Remnants of subduction zones and oceanic basins that composed the once vast Neotethyan Ocean are scattered along the suture zone between India and Eurasia (e.g., Hébert et al., 2012, Figure 1). The origin and evolution of these tectonic elements often remain unclear because of data gaps regarding their age, provenance, and paleo-tectonic settings. The lack of constraints as to how India-Eurasia convergence was accommodated during the Cretaceous-early Cenozoic impedes the understanding of processes and timescales that govern the evolution of convergent plate boundaries (Aitchison, Ali, & Davis, 2007; Guillot et al., 2003; Hafkensheid et al., 2006; Jagoutz et al., 2015; Kapp & DeCelles, 2019; van Hinsbergen et al., 2018).

Whether a Neotethyan intraoceanic arc existed between India and Eurasia and, if it did, whether it collided first with India or Eurasia represent large uncertainties in constraining the magmatic and tectonic evolution of the India-Eurasia convergent system (e.g., Aitchison, Ali, & Davis, 2007; Hu, Wang, et al., 2016; Parsons et al., 2020). In particular, Mesozoic igneous and volcaniclastic rocks in Ladakh have been interpreted as resulting from the activity of a single Eurasian Andean-style arc (Dras-Kohistan-Ladakh arc; for example, Dietrich et al., 1983; Garzanti & Van Haver, 1988) or a combination of a Eurasian Kohistan-Ladakh arc and an exotic Spong intraoceanic arc,

© 2022 The Authors.

This is an open access article under the terms of the [Creative Commons Attribution-NonCommercial License](https://creativecommons.org/licenses/by-nc/4.0/), which permits use, distribution and reproduction in any medium, provided the original work is properly cited and is not used for commercial purposes.

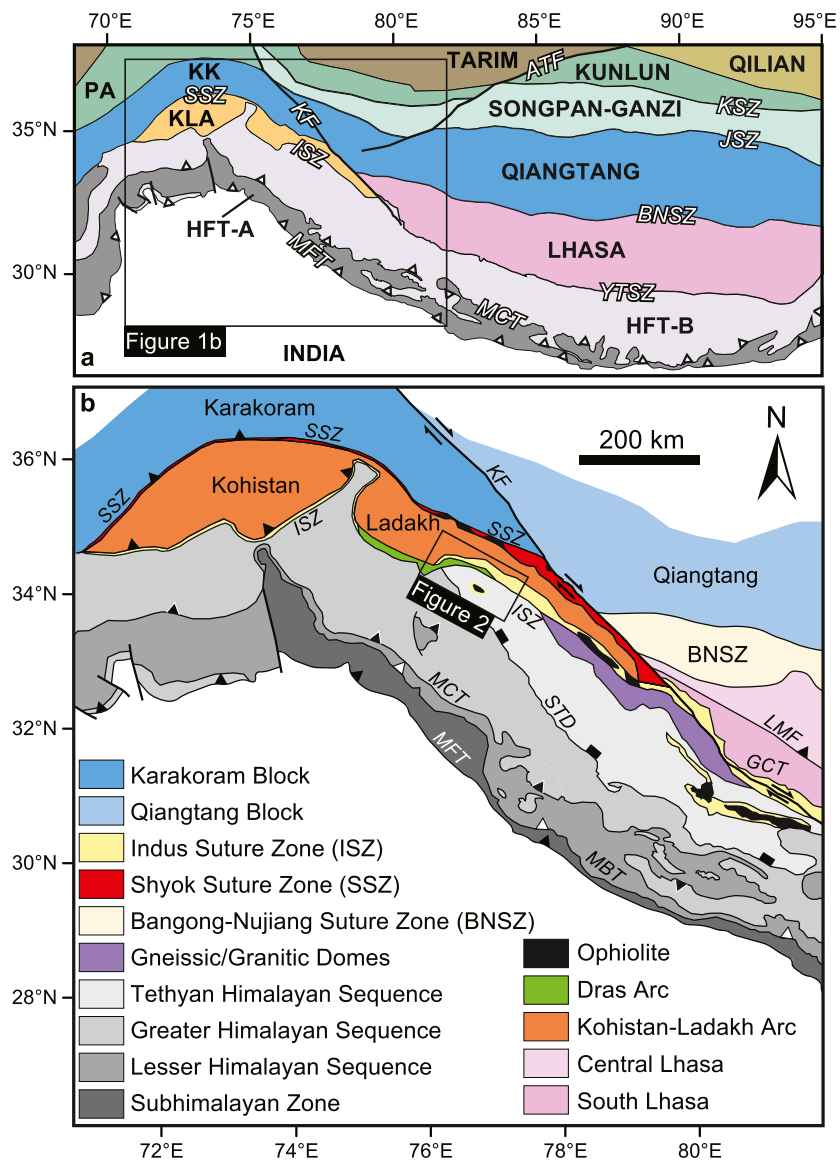


**Figure 1.** (a) Terrane map of major crustal blocks and tectonic boundaries of the Himalayan orogen (modified after Parsons et al., 2020). (b) Simplified geological map of the western Himalayan orogen (modified after Parsons et al., 2020). Blocks: HFT-A = Himalaya Fold-and-Thrust Belt, Sequence A; HFT-B = Himalaya Fold-and-Thrust Belt, Sequence B; KK = Karakoram; KLA = Kohistan-Ladakh; PA = Pamir. Tectonic structures: ATF = Altyn Tagh Fault; BNSZ = Bangong-Nujiang Suture Zone; GCT = Great Counter Thrust; ISZ = Indus Suture Zone; JSZ = Jinsha Suture Zone; KF = Karakoram Fault; KSZ = Kunlun Suture Zone; LMF = Luobadui-Milashan Fault; MCT = Main Central Thrust; MFT = Main Frontal Thrust; SSZ = Shyok Suture Zone; STD = South Tibetan Detachment; YTSZ = Yarlung Tsangpo Suture Zone.

both of which may have hosted the Dras arc (e.g., Buckman et al., 2018; Corfield et al., 1999; Mahéo et al., 2004; Reuber, 1989; Robertson & Degnan, 1994; Walsh et al., 2019). In scenarios where two separate magmatic arcs are invoked, the Neotethyan intraoceanic arc is proposed to either collide first with India (75 Ma in Corfield & Searle, 2000; 55 Ma in Buckman et al., 2018) or with Eurasia (83.5–93.5 Ma in Clift, Hannigan, et al., 2002; 65 Ma in Mahéo et al., 2006). A subset of studies considers that the Kohistan-Ladakh arc was the prototypical Neotethyan intraoceanic arc, which collided first with India (61 Ma in Khan et al., 2009; 50 Ma in Bouilhol et al., 2013; Martin et al., 2020) or with Eurasian Karakoram (Late Cretaceous; Borneman et al., 2015; Clift et al., 2000; Henderson et al., 2010; Robertson & Degnan, 1994; Rolland, 2002). Moreover, contradicting views exist as to the nature of the along-strike continuity of the Neotethyan intraoceanic arc during the Mesozoic,

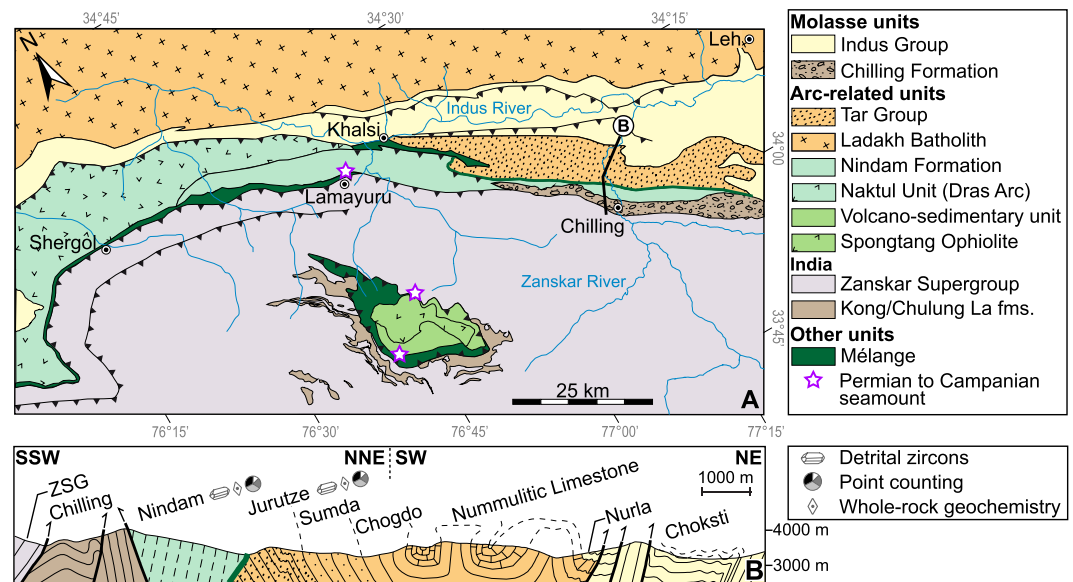


**Figure 2.** (a) Geological map of NW Ladakh, India (modified after Buckman et al., 2018; Clift, Carter, et al., 2002; Corfield & Searle, 2000; Fuchs, 1986; Henderson et al., 2010, 2011; Steck, 2003). Fms. = formations. (b) Cross-section modified after Henderson et al. (2010, 2011). ZSG = Zaskar Supergroup.

with proposed connections with Lhasa Block (e.g., Parsons et al., 2020; Rolland et al., 2000), India (e.g., Walsh et al., 2019), or Australia (Hall, 2012). This large set of mutually exclusive views complicates the correlation of subduction zone remnants along the Himalayan orogen and thus obscures the location of ancient plate boundaries and the size of the tectonic elements within the Tethyan realm.

We explore the tectono-stratigraphic links between the fault-bounded middle Cretaceous to lower Cenozoic Nindam and Jurutze volcanoclastic formations, which are exposed in the Indus Suture Zone in Ladakh (India). New sedimentary, petrographic, whole-rock geochemical, and zircon geochronological and geochemical data from marine volcanoclastic rocks provide an opportunity to constrain the depositional ages and provenance of these units, and their source-to-sink relationships with the Dras and Kohistan-Ladakh arcs.

## 2. Geological Background

The Indus Suture Zone in NW Ladakh is composed of igneous and sedimentary units (Figures 1–3). Exposed north of the suture zone are the Upper Jurassic to Eocene intrusive and volcanic units of the Kohistan-Ladakh arc, which consists mainly of the Uppermost Cretaceous to Eocene Ladakh Batholith in the study area (Bouilhol et al., 2013; Heri et al., 2015; Jagoutz et al., 2019; Lakhan et al., 2020a, 2020b; Ravikant et al., 2009; Saktura et al., 2020; Shellnutt et al., 2014; White et al., 2011). The post-lower Eocene Indus Group consists of alluvial and fluvial deposits that unconformably overlie the southern margin of the Ladakh Batholith (Fuchs, 1979; Garzanti & Van Haver, 1988; Henderson et al., 2010; Searle et al., 1990; Zhou et al., 2020). Further to the south, the Indus Group conformably overlies the middle Cretaceous to lower Eocene Tar Group, which consists of the Aptian–Albian Khalsi Limestone, the upper Albian to lower Eocene deep-water volcanoclastic Jurutze Formation, the lower Eocene shelfal Sumda Do Formation, the fluvial Chogdo Formation, and the lower Eocene shallow-water Nummulitic Limestone (Clift, Carter, et al., 2002; Garzanti & Van Haver, 1988; Green et al., 2008; Henderson et al., 2010, 2011; Searle et al., 1990). The nature of the contact between the Tar Group and the Ladakh Batholith is unknown. The Tar Group is generally considered as the forearc basin of the Kohistan-Ladakh arc (Garzanti & Van Haver, 1988; Henderson et al., 2010; Wu et al., 2007). The Upper Jurassic to Paleocene Dras intraoceanic arc is tectonically juxtaposed against the Ladakh Batholith, the Tar Group and the Indus Group, to the north, and thrust over the Indian passive margin, to the south. The western part of the Dras arc is dominated by mafic to intermediate volcanic rocks, which transition eastwards into the deep-water volcanoclastic

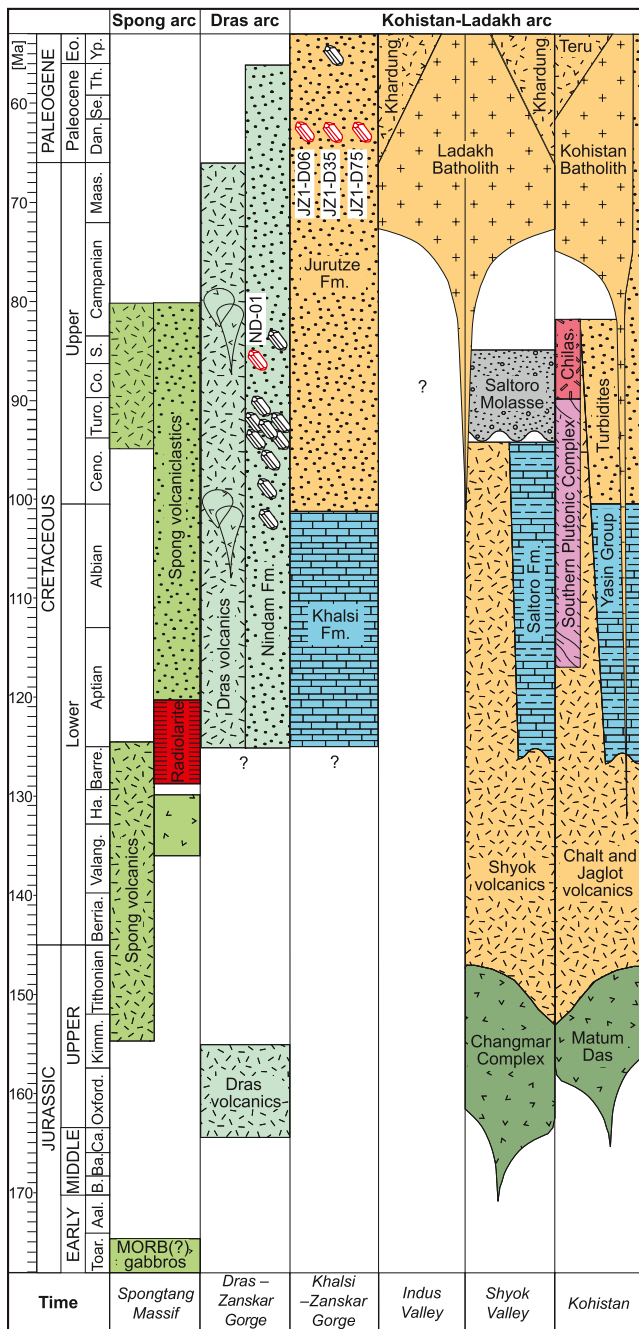


**Figure 3.** Chronostratigraphic chart of the Spong, Dras and Kohistan-Ladakh arcs (modified after Garzanti & Van Haver, 1988; Robertson & Degnan, 1994; Saktura et al., 2020; Upadhyay et al., 2004; Walsh et al., 2019, 2020). Detrital zircon samples: this study (in red); previous studies (in black): Jurutze, Henderson et al., 2010; Nindam, Walsh et al., 2019).

rocks of the Aptian to Paleocene Nindam Formation (Bhat et al., 2019; Clift et al., 2000; Clift, Hannigan, et al., 2002; Dietrich et al., 1983; Honegger et al., 1982; Reuber, 1989; Robertson & Degnan, 1994; Steck, 2003; Suture, 1990; Upadhyay et al., 2004; Walsh et al., 2019, 2020). Exposed south of the suture zone is the Permian to lower Eocene Zaskar Supergroup of the Tethyan Himalaya (northern Indian margin), which is thrust under the Jurassic to Upper Cretaceous Spong tang supra-subduction zone ophiolite (Buckman et al., 2018; Corfield & Searle, 2000; Mahéo et al., 2004; Najman et al., 2017; Nicora et al., 1987; Reuber et al., 1987; Steck, 2003). Ophiolitic detritus-bearing, lower to middle Eocene sedimentary rocks of the Tethyan Himalaya are in tectonic contact with the Dras arc and the Spong tang ophiolite (Kong, Chulung La, and Chilling formations; Baxter et al., 2016; Buckman et al., 2018; Fuchs, 1986; Garzanti et al., 1987; Najman et al., 2017).

In northern Ladakh, the Shyok Suture Zone separates the Kohistan-Ladakh arc from the Gondwana-derived Karakoram Block (Coward et al., 1986; Pudsey, 1986; Rolland et al., 2000). The latter records Paleozoic–Mesozoic sedimentation (Gaetani, 1997; Rolland, Picard, Pêcher, Carrio, et al., 2002) on a >651 Ma Precambrian basement (Rolland et al., 2006b), Late Triassic to Miocene phases of magmatism (Borneman et al., 2015; Heuberger et al., 2007; Kumar et al., 2017; Phillips et al., 2013; Ravikant et al., 2009; Rolland et al., 2001, 2006b; Searle et al., 1989, 2010), Early to Late Jurassic and Early to Late Jurassic Cretaceous phases of deformation (Gaetani et al., 1990, 1993), and middle Cretaceous to Cenozoic metamorphic events (Rolland et al., 2006a; Searle & Hacker, 2019). The Karakoram and Qiangtang blocks, as well as the suture zones (Shyok and Bangong) bounding their southern margins, are considered correlative across the Karakoram Fault (Baxter et al., 2009; Borneman et al., 2015; Phillips et al., 2004; Robinson, 2009; Rolland et al., 2009). In contrast to the consensus that the Bangong suture is Cretaceous in age, the closure timing along the Shyok suture is debated. Geologic, metamorphic, and stratigraphic data from the Shyok suture and adjacent Karakoram Block support a middle Cretaceous accretion of the Kohistan-Ladakh arc (Borneman et al., 2015; Kumar et al., 2017; Palin et al., 2012; Rex et al., 1988; Rolland et al., 2000; Treloar et al., 1989), whereas geochemical and paleomagnetic data from the Kohistan-Ladakh arc are possibly indicative of a collision with India at ca. 50 Ma and a later collision with Karakoram at ca. 40 Ma (Bouilhol et al., 2013; Martin et al., 2020).

The eastward correlation of the Kohistan-Ladakh and Dras arc remnants with Tibetan units is controversial. Arc remnants from Ladakh are commonly correlated with those of the Lhasa Block, which consists of a Precambrian basement overlain and intruded by Paleozoic to Cenozoic strata and magmatic rocks (Dürr, 1996; Zhu et al., 2009). This correlation is based on the similar age, structural position, and geochemistry of the Late Cretaceous–Cenozoic batholiths from both areas (Gangdese, Ladakh, Kohistan; Ji et al., 2009; Raz & Honegger, 1989; Rolland et al., 2000; Wang et al., 2012; Weinberg et al., 2000). In contrast, the Precambrian and Paleozoic rocks of the Lhasa Block have no equivalent in the Kohistan-Ladakh and Dras arc remnants. Alternative connections were proposed between intraoceanic arc remnants located south of the Lhasa Block (Zedong arc; Aitchison et al., 2000; Aitchison et al., 2007; McDermid et al., 2002) and either the Kohistan-Ladakh arc (Parsons et al., 2020), the Dras arc (e.g., Walsh et al., 2020), or the Spong arc (e.g., Hébert et al., 2012).

In summary, existing data from Ladakh define at least three possible sources for the Cretaceous to lower Cenozoic volcaniclastic rocks exposed in the Indus Suture Zone: (a) the Karakoram Block; (b) the Kohistan-Ladakh

arc; (c) and the Dras arc (Figure 1b). The occurrence of these sources in the Nindam and Jurutze formations is tested below with the analysis of detrital zircons (DZ) and tuffaceous beds from the Zanskar Gorge (Figure 2). Whether sources from blocks located farther away (e.g., Tibet) played a role in the provenance of these rocks needs to be tested and substantiated with additional data.

### 3. Sampling Strategy and Methods

We used three complementary methods to constrain the provenance of the Nindam and Jurutze formations (Figure 2). The Nindam Formation was studied between  $N34^{\circ}03'16.0''/E77^{\circ}12'41.2''$  and  $N34^{\circ}03'35.6''/E77^{\circ}12'38.3''$ , whereas the Jurutze Formation was logged and sampled between  $N34^{\circ}05'43.2''/E077^{\circ}12'40.8''$  and  $N34^{\circ}05'45.3''/E077^{\circ}12'46.1''$  (see detailed log of the 100 m thick section in Figure S1 in Supporting Information S1). The nature and exact location of the contact between the Nindam and Jurutze formations remains poorly identified, which is due to the faulting and tight folding that commonly affects both formations, as well as to poor exposure related to scree slopes within the gorge. Moreover, both formations contain greyish thin-bedded, laminated, hemipelagic mudstones and siltstones, further complicating the identification of a clear contact between them. This uncertainty was already reflected in competing geological maps of the Zanskar Gorge whereby either (a) stratigraphic continuity (e.g., Clift et al., 2000; Henderson et al., 2011; Searle et al., 1990) or (b) a tectonic limit (e.g., thrust fault in Clift, Carter, et al., 2002; serpentinite mélange in Steck, 2003; see Figure 2) are inferred between the Jurutze and Nindam formations. We choose to examine the Nindam Formation close to its fault bounded southern contact with the Chilling Formation and the Jurutze Formation close to its depositional northern contact with the Sumda Do Formation (see coordinates above). We combine DZ ages and geochemical data, sandstone modal compositions, and whole-rock geochemistry on tuffaceous beds to constrain the ages and provenance of the Jurutze and Nindam formations.

The modal compositions of four sandstones from the Nindam Formation and three sandstones from the Jurutze Formation were determined using the point-counting method of Dickinson and Suczek (1979). The counted grains correspond to monocrystalline quartz, polycrystalline quartz, plagioclase, and K-feldspar. Fragments of volcanic rocks are the only type of unstable lithic fragment observed in the samples.

We analyzed the major and trace element whole-rock compositions of five tuffaceous rocks from the Jurutze Formation and three tuffaceous rocks from the Nindam Formation. We analyzed carbonate-free, fine ash-rich beds ( $<62.5 \mu\text{m}$  particles) because they are chiefly composed of volcanic glass, the accumulation of which is expected to have occurred shortly after eruption events due to its rapid chemical and mechanical weathering (Schacht et al., 2008). Although possibly biased toward the more silicic explosive volcanic outputs, the geochemistry of tuffaceous beds is otherwise expected to mimic that of coeval magmatic rocks (Clift et al., 2000; Robertson et al., 2018; Schindlbeck et al., 2018). Coarser rocks were avoided because there are more likely to have incorporated a mixture of components from various sources, which could result in ambiguous geochemical signatures.

DZ geochronology was performed using laser ablation ICP-MS on three samples of the Jurutze Formation and one sample from the Nindam Formation. The analytical procedure presented here is similar to that of Zhou et al. (2020). We dated 807 grains from four samples at the Centre for Geoanalytical Mass Spectrometry, School of Earth and Environmental Sciences, The University of Queensland. Trace elements were measured on a subset of these grains, which includes 110 grains from two samples of the Jurutze Formation and 123 grains from one sample of the Nindam Formation. Additional details on the analytical methods are included in File S2 in Supporting Information S1.

## 4. Results

### 4.1. Lithology and Sandstone Petrography

In the Zanskar Gorge, the deep-water Jurutze and Nindam formations are composed of greyish-greenish clay-to sand-sized volcanoclastic turbidites (Figure 3). The Nindam Formation typically displays decimeter to meter-sized green sandstone beds, which locally alternate with centimeter-sized green to greyish, laminated, radiolarian-bearing mudstone and siltstone beds. In contrast, the Jurutze Formation is dominated by centimeter-sized greyish, laminated mudstone and siltstone beds, with subordinate centimeter to decimeter-sized greyish to greenish sand-

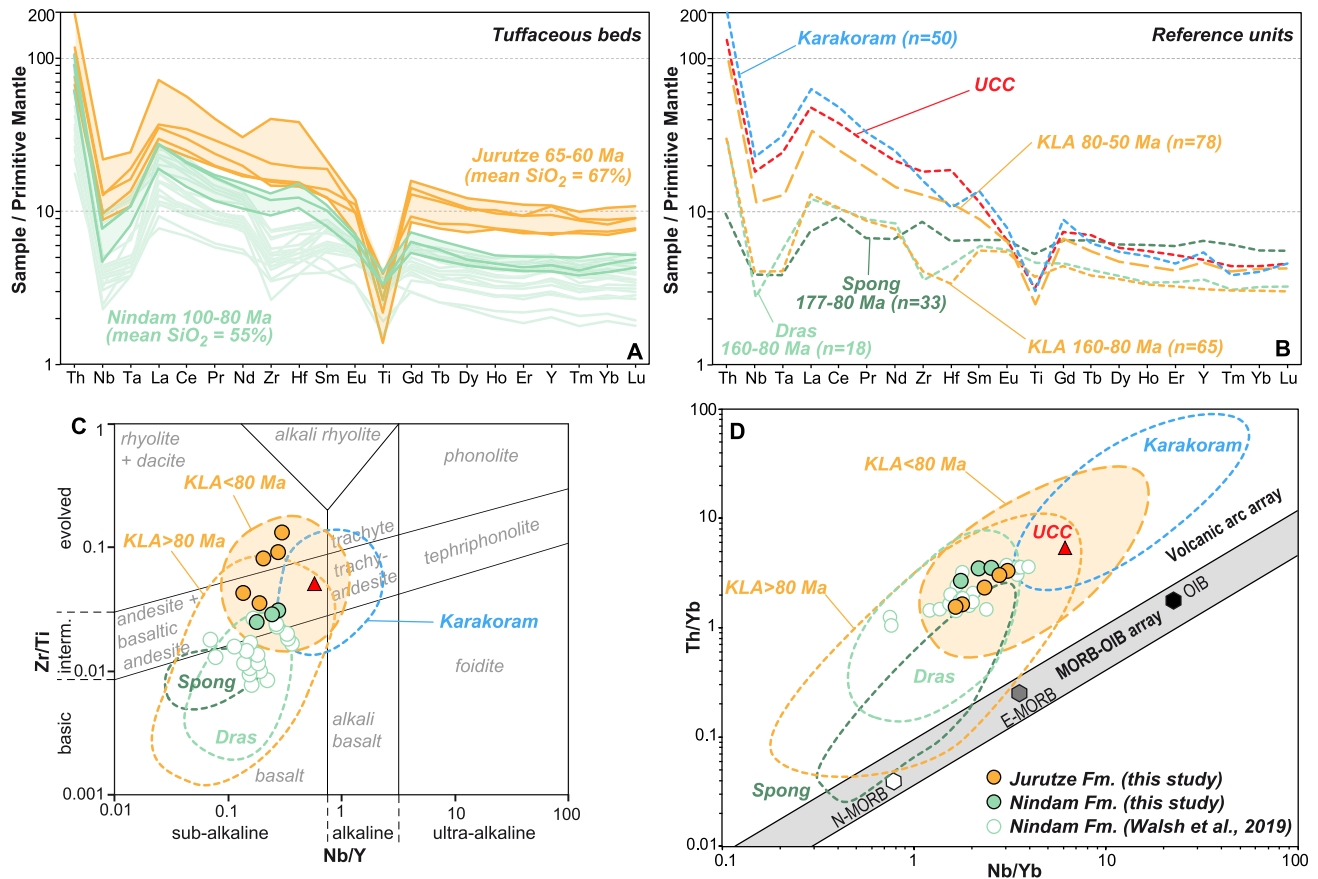


**Figure 4.** Whole-rock geochemistry of tuffaceous beds from the Jurutze and Nindam formations (Zaskar Gorge, NW Ladakh, India). (a) Primitive mantle-normalized multielement diagram. The lighter colored green lines of the Nindam Formation are from Walsh et al. (2019). The  $\text{SiO}_2$  average of the Nindam Formation is based on new (Table S4 in Supporting Information S1) and existing data (File S1 in Supporting Information S1). (b) Primitive mantle-normalized multielement diagram displaying the Jurutze and Nindam formations in comparison with the average compositions of arc-related units exposed in Ladakh. Data sources are listed in the Supplementary Materials (File S1 in Supporting Information S1). (c)  $\text{Zr/Ti}$  versus  $\text{Nb/Y}$  discrimination diagram from Pearce (1996). (d)  $\text{Nb/Y}$  versus  $\text{Th/Yb}$  discrimination diagram from Pearce (2008). Primitive mantle after McDonough and Sun (1995). Upper continental crust (UCC) after Rudnick and Gao (2003).

stones. Sandstones of both formations are dominated by lithic grains, with minor proportions of feldspars and quartz (ca. Q6%F17%L77%; Figures S2 and S3, Table S1 in Supporting Information S1). Lithic components correspond to fragments of vitric tuff displaying glassy to microcrystalline textures, which is typical of sediments deposited close to active magmatic arcs (Draut & Clift, 2006). Except for a possible slightly higher proportion of quartz, the sandstones of the Jurutze Formation show no clear petrographic difference with that of the Nindam Formation in the Zaskar Gorge.

#### 4.2. Major- and Trace-Element Geochemistry

Tuffaceous beds of the Jurutze and Nindam formations show distinct geochemical compositions (Figure 4, Table S4 in Supporting Information S1). The Nindam Formation ranges from basaltic trachyandesite to andesite in composition (55%–59%  $\text{SiO}_2$ ), whereas the rocks of the Jurutze Formation are mostly dacitic with subordinate trachyandesite and rhyolite compositions (58%–78%  $\text{SiO}_2$ ). In normalized trace element diagrams both formations have supra-subduction signatures with Nb-Ta and Ti negative anomalies. In a  $\text{Nb/Y}$  versus  $\text{Th/Yb}$  diagram (Pearce, 2008), the Jurutze and Nindam formations plot in the volcanic arc array and present similar ratios. When compared to the Nindam Formation, the relatively higher  $\text{SiO}_2$  contents of the Jurutze Formation are consistent with: (a) higher differentiation index values ( $\text{Zr/Ti}$ ; Pearce, 1996); (b) and significantly higher trace element contents.

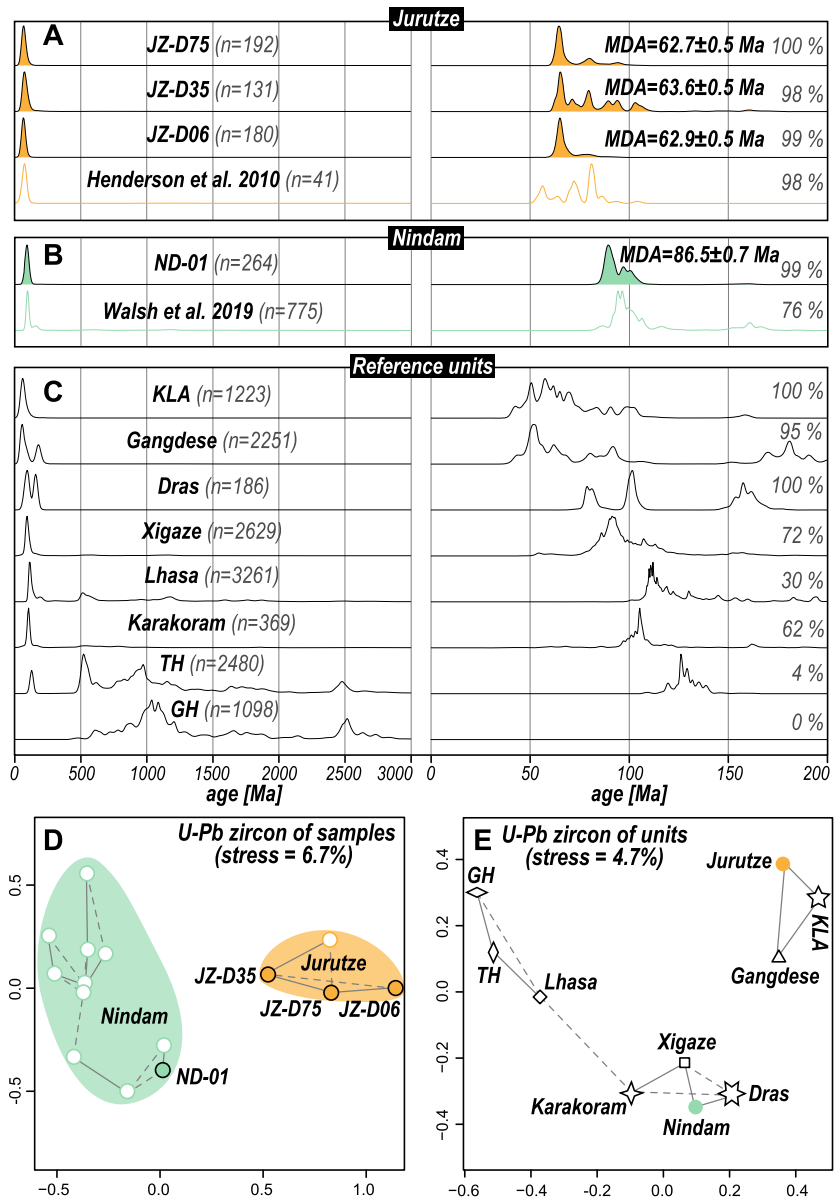


**Figure 5.** U-Pb DZ ages from the Jurutze and Nindam formations (Zaskar Gorge, NW Ladakh, India) and selected bedrock terranes. (a), (b) Kernel density estimates (KDE) of U-Pb DZ ages from the Jurutze (JZ-D06, JZ-35, JZ-D75) and Nindam (ND-01) formations. New data are compared to composite samples from previous studies discussed in the main text. YC2σ(3+) of Dickinson and Gehrels (2009) is used to infer DZ maximum depositional ages (MDA). (c) KDE of selected bedrock sources terranes. Datasets from the literature are listed in File S1 in Supporting Information S1. (d), (e) Nonmetric multidimensional scaling (MDS) plots showing the Kolmogorov-Smirnov distances (d) between individual Nindam and Jurutze samples and (e) among composite Nindam and Jurutze samples and bedrock source terranes. New samples in (d) shown by full circles. Statistical similarity represented by closeness of datapoints, where solid lines indicate closest neighbors and dashed lines indicate near neighbors. Stress, a “goodness-of-fit” parameter for MDS, of less than 10% is considered “good” for moderate to large datasets (Vermeesch et al., 2016).

### 4.3. DZ U-Pb Geochronology

New DZ samples ( $N = 3$ ,  $n = 503$ ) from the Jurutze Formation show a major peak at 65 Ma and lesser peaks at 75, 80, 93, 103, 144, and 161 Ma (Figure 5a; detailed geochronology results are provided in Tables S2 and S3 in Supporting Information S1). Detrital populations are Cenozoic (45.5%), Late Cretaceous (48.3%), Early Cretaceous (3.8%), Jurassic (1.6%), and Precambrian (0.8%) in age. The single youngest zircon of our data

set has an age of  $55.1 \pm 1.3$  Ma ( $2\sigma$ , late Thanetian–early Ypresian), similar to the single youngest zircon age ( $53.4 \pm 1.4$  Ma) reported from a higher stratigraphic level (Henderson et al., 2010). However, more robust calculations of the maximum depositional age—expressed as  $YC2\sigma(3+)$  (mean age of the youngest cluster ( $n \geq 3$ ) of grain ages that overlap in age at  $2\sigma$ ; Dickinson & Gehrels, 2009)—for each sample consistently provide older ages at ca. 63 Ma, which supports a Danian age rather than a late Thanetian–early Ypresian age of the studied section.

New DZ ( $N = 1$ ;  $n = 264$ ) from the Nindam Formation show major peaks at 89 and 97 Ma and lesser peaks at 153 and 160 Ma (Figure 5b). Detrital populations are Late Cretaceous (82.2%), Early Cretaceous (13.2%), Jurassic (3.4%), Triassic (0.4%), and Precambrian (0.8%) in age. The single youngest zircon of our new sample has an age of  $84.1 \pm 1.7$  Ma ( $2\sigma$ , Santonian). A more robust calculation of the maximum depositional age provides a slightly older age at  $86.5 \pm 0.7$  Ma ( $YC2\sigma(3+)$ , late Coniacian–early Santonian). This maximum depositional age is ca. 23 m.y. older than that obtained for the adjacent Jurutze Formation.

#### 4.4. Detrital Zircon Geochemistry

Trace elements were analyzed from a subset of DZ from the Nindam ( $n = 123$ ) and Jurutze ( $n = 110$ ) formations (Figure 6; detailed *in-situ* geochemistry results are provided in Table S3 in Supporting Information S1). DZ from both formations share similar low to medium U/Yb, Nb/Yb, and Hf contents, which are compatible with a relatively primitive magmatic arc setting. Trace element ratios such as Yb/Gd, Sc/Yb, Th/U, Nb/Sc, and Lu/Hf show that DZ compositions of the Jurutze Formation: (a) at ca. 65 Ma overlap partly that of the Nindam Formation at ca. 90 Ma; (b) define enrichment/depletion trends between ca. 100 and 65 Ma; (c) are similar to those of coeval DZ of the Nindam Formation in the 100–85 Ma interval. In particular, some Sc/Yb, Th/U and Lu/Hf values of the Nindam and Jurutze formations in the 100–85 Ma interval do not overlap with those of the post-85 Ma Jurutze Formation. Moreover, the Nindam and Jurutze formations have a very narrow range of Nb/Sc values in the 100–85 Ma interval, which is not observed in the post-85 Ma Jurutze Formation. Although additional geochemical data are needed to better characterize this component, it is noteworthy that ca. 160 Ma zircons in the Nindam and Jurutze formations have a similar composition to that of post-110 Ma zircons.

### 5. Discussion

#### 5.1. Age and Provenance of the Nindam and Jurutze Formations in the Zaskar Gorge

The results presented here show that, in the Zaskar Gorge, the Paleocene Jurutze and Upper Cretaceous Nindam formations have dissimilar maximum depositional ages (ca. 63 Ma vs. ca. 86 Ma) and whole-rock geochemical compositions (Figures 4a and 5d). This agrees with previous field observations that were used to infer a tectonic separation between these formations along a thrust fault or a serpentinite mélange (Clift, Carter, et al., 2002; Steck, 2003, Figure 2). Such a tectonic separation was clearly established near Khalsi (e.g., Robertson & Degnan, 1994; Walsh et al., 2019) and mapped between Khalsi and the Zaskar Gorge (Steck, 2003). This rules out a depositional contact existing between these formations as previously suggested in several studies (Clift et al., 2000; Henderson et al., 2011; Searle et al., 1990).

DZ ages from the Jurutze Formation are consistent with a derivation from the Kohistan-Ladakh arc, which presents major peaks at 50, 58, 62, and 65 Ma, and lesser peaks between 80 and 159 Ma (Figure 5). The low proportion of Jurassic zircons in the Jurutze Formation (1.6%) is comparable to that of the Kohistan-Ladakh arc (2.7%). Major and trace element compositions of the Jurutze Formation overlap that of the 80–50 Ma igneous rocks of the Kohistan-Ladakh arc (Figure 4). This interpretation is in agreement with previous studies (e.g., Clift, Carter, et al., 2002; Garzanti & Van Haver, 1988; Henderson et al., 2010) that consider the Jurutze Formation as the forearc basin to the Kohistan-Ladakh arc.

DZ ages, whole-rock geochemical data and sandstone QFL compositions of the Nindam Formation in the Zaskar Gorge (this study) are mostly consistent with those of the Nindam Formation in the Yapola Valley near Lamayuru (Figures 3 and 4; Walsh et al., 2019). The bulk of the Nindam Formation has detrital populations that fit the igneous zircon ages of the Dras arc (this study; Walsh et al., 2020, Figure 5), with common peaks at ca. 100 and 160 Ma. These affinities are consistent with the maps of Robertson and Degnan (1994) and Steck (2003), where the Nindam Formation is mapped between the Yapola Valley and the Zaskar Gorge and is regarded as a forearc succession to the Dras arc. Based on overlapping zircon ages, the Nindam Formation may have also been sourced



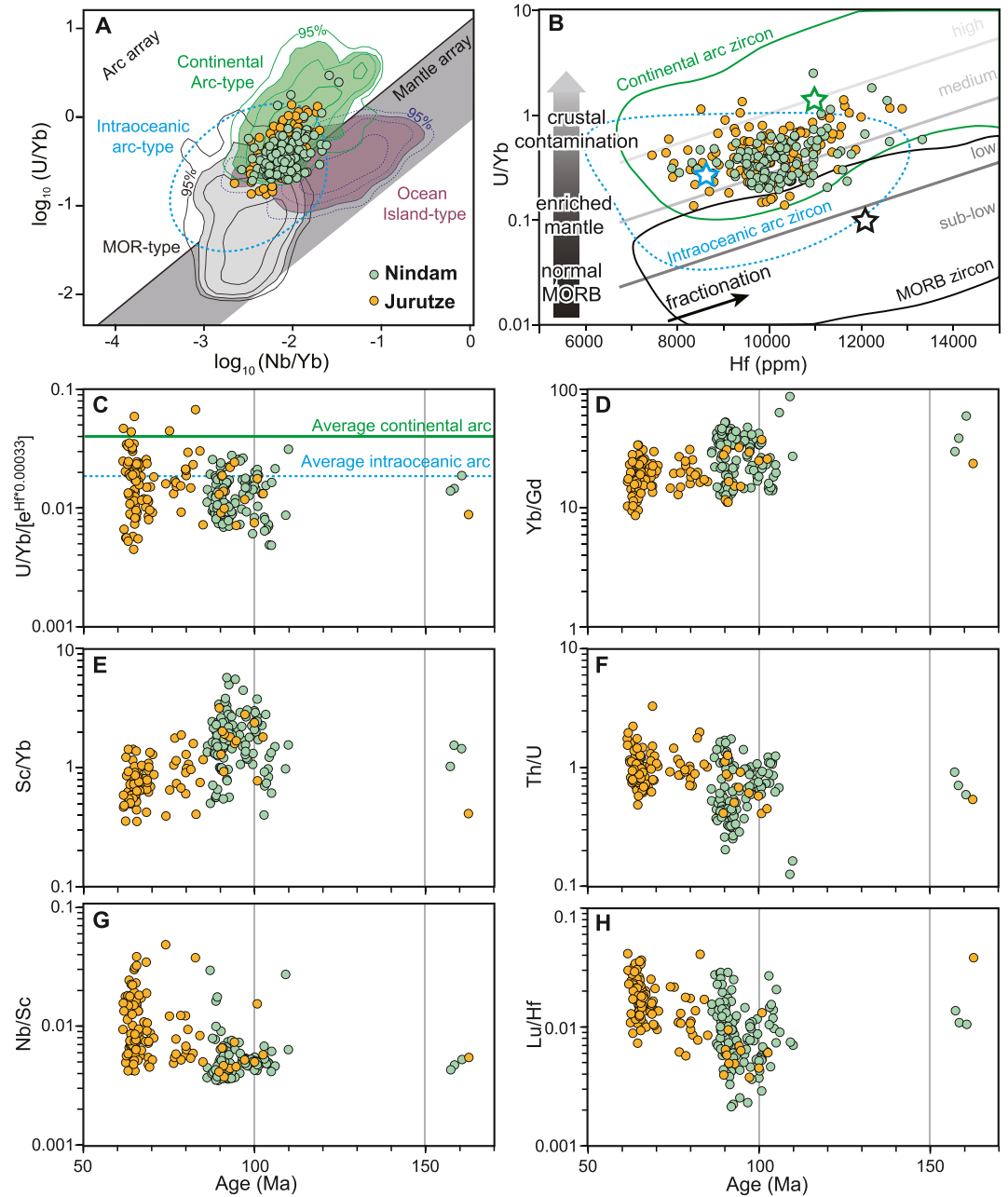


**Figure 6.** Trace element composition of Zr from the Jurutze and Nindam formations (Zaskar Gorge, NW Ladakh, India). (a) Nb/Yb versus U/Yb discrimination diagram after Grimes et al. (2015). (b) Hf versus U/Yb diagram modified after Johnston and Kylander-Clark (2021). The stars represent average values of the reference settings. (c)–(h) Zr age versus selected trace element ratios. In (c), Hf-corrected U/Yb calculation after Johnston and Kylander-Clark (2021). (a)–(c) Intraoceanic arc zircon values from: Barth et al. (2017), Grimes et al. (2015), Kay et al. (2019), Schmitt et al. (2018). (b), (c) Continental arc zircon values from Grimes et al. (2015).

from the Karakoram Block, but such a source is unlikely because its trace element and isotopic compositions are distinct from those of the Nindam Formation (Clift, Hannigan, et al., 2002, Figure 4).

## 5.2. Common Features of the Dras and Kohistan-Ladakh Arcs

Our results confirm previous views of a derivation of the Nindam and Jurutze formations from the Dras and Kohistan-Ladakh arcs, respectively. However, there is still a debate as to whether these units were formed at the

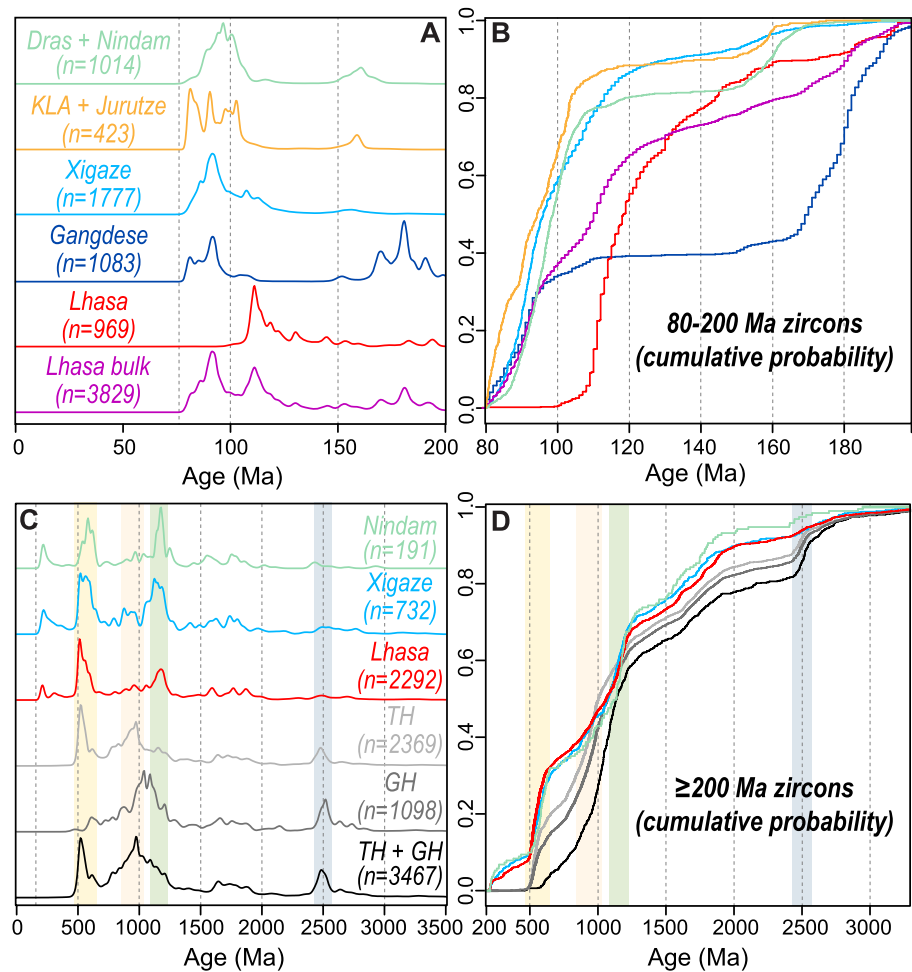


**Figure 7.** (a), (c) Kernel density estimations (KDE) and (b), (d) cumulative probability plots of U-Pb zircon ages. (a), (b) Age distributions of the 80–200 Ma (Jurassic to Late Cretaceous) zircons from the Jurutze and Nindam formations in combination with those of the Dras and Kohistan-Ladakh (KLA) arcs, respectively. The age distribution of Dras + Nindam is similar to KLA + Jurutze in that interval. In (c), (d) the age distribution of the Nindam Formation is similar to Lhasa and Xigaze in the 200–3,500 Ma interval (Paleoproterozoic to Triassic). Datasets same as listed in Figure 5, with the following units merged here: Dras + Nindam; KLA + Jurutze; Lhasa bulk = Gangdese + Lhasa (central and northern) + Xigaze. In (c) and (d), the color bands highlight important ages peaks.

same convergent margin (e.g., Buckman et al., 2018; Clift et al., 2000; Garzanti & Van Haver, 1988; Parsons et al., 2020; Robertson, 2000; Robertson & Degan, 1994; Walsh et al., 2019, 2020). Placement of these arc remnants along a single convergent margin has remained speculative because previous studies lacked piercing lines that could reconnect the arc-related rocks from the Indus Suture Zone with those exposed to the north. Up to now, the main argument in favor of a single Dras-Kohistan-Ladakh arc has been the 103–101 Ma Kargil intrusive, which intruded the Dras arc volcanics and may be interpreted as an equivalent of the Ladakh Batholith (Bouilhol et al., 2013; Honegger et al., 1982; Steck, 2003). In the next sections, we show that striking similarities actually exist between the Dras and Kohistan-Ladakh arcs when data from the same time interval (i.e., ca. 80–200 Ma) are compared. Based on new and existing data, we discuss three piercing lines supporting the Dras and Kohistan-Ladakh arcs having been part of a single convergent margin.

### 5.2.1. Zircon Age Distributions

Figures 7a and 7b shows a compilation of zircon ages from igneous and detrital rocks where the Nindam and Jurutze formations are merged with the Dras and Kohistan-Ladakh arcs, respectively. The Dras + Nindam and Kohistan-Ladakh + Jurutze units share almost identical zircon age distributions in the 80–200 Ma interval, with a prominent peak at ca. 100 Ma and a smaller peak at ca. 160 Ma. This age distribution is distinct from that of

all other units used for comparison (Figures 5c, 7a and 7b). Moreover, both zircon age distributions feature a time interval (150–120 Ma) with very few zircon ages, which is 9 out of 423 zircons (ca. 2.1%; uncertainties not considered) for the Kohistan-Ladakh + Jurutze unit and 26 out of 1,013 zircons (ca. 2.5%) for the Dras + Nindam unit. Whether this represents a lull in the volcanic activity of these arcs or undersampling of 150–120 Ma zircons remains unknown. Although having a different zircon age distribution, the Gangdese belt is characterized by a similar age gap (Figure 7).

### 5.2.2. DZ Geochemistry

Our geochemical results on DZ from the Nindam and Jurutze formations provide an additional link between them and, by extension, between the Dras and Kohistan-Ladakh arcs. Despite a significant difference in depositional age in the Zaskar Gorge, the Nindam and Jurutze DZ have overlapping low to medium U/Yb, Nb/Yb, and Hf contents which suggest that they were sourced from a similar magmatic arc setting. These compositions are compatible with both intraoceanic and continental arc settings, but high U/Yb zircons typical of long-lived continental arcs are very scarce (Figure 6). Importantly, additional trace element ratios show that DZ from the Jurutze Formation have temporal enrichment/depletion trends, which overlap DZ compositions of the Nindam Formation in the 100–85 Ma interval. Moreover, decreasing Yb/Gd and increasing Th/U values through time are consistent with the magmatic evolution of a single convergent margin (Barth et al., 2013). Increasing chondrite-normalized Gd/Yb values of igneous rocks of the Kohistan-Ladakh arc from 118 to 60 Ma (Jagoutz et al., 2019) are consistent with those of the Jurutze and Nindam DZ. Whether these are indicative of an overall crustal thickening through time remains to be further tested in future studies.

### 5.2.3. Whole-Rock Geochemistry

As discussed above and shown in Figure 4, the enriched primitive mantle-normalized multielement patterns of the Paleocene Jurutze Formation are consistent with the average composition of the post-80 Ma Kohistan-Ladakh arc. In contrast, the more primitive composition of the Upper Cretaceous Nindam Formation is consistent with that of the 160–80 Ma Dras arc (Clift, Hannigan, et al., 2002; Walsh et al., 2019; this study). Besides being indicative of distinct SiO<sub>2</sub> contents of source rocks, these contrasting geochemical compositions of tuffaceous rocks are in reality consistent with the overall geochemical evolution of the Kohistan-Ladakh arc from 160 to 50 Ma. In other words, the trace element geochemistry of 160–80 Ma igneous and sedimentary rocks of the Dras arc is indistinguishable from that of the 160–80 Ma igneous rocks of the Kohistan-Ladakh arc. The post-80 Ma change to more enriched trace element compositions in the Kohistan-Ladakh arc (e.g., Jagoutz et al., 2019) is a feature commonly described in other intraoceanic arcs shifting from primitive to mature stages (e.g., Costa Rica, Gazel et al., 2019; Aleutians, Kay et al., 2019; Izu Bonin, Saito & Tani, 2017), although the causes of such a compositional shift may differ from one arc setting to the other.

## 5.3. DZ Connection Between the Dras Arc and Lhasa?

Walsh et al. (2019) documented significant amounts of pre-Cretaceous DZ in middle to Upper Cretaceous strata of the Nindam Formation, which they suggested reflected a derivation from the Indian continent. This Gondwanan inheritance was used to constrain a model of intraoceanic arc subduction initiation in the vicinity of India, which explains the inferred development of sedimentary pathways between India and the Dras arc.

In Figures 7c and 7d, the age distribution of the pre-200 Ma DZ from the Nindam Formation shows two major peaks at 584 Ma and 1,177 Ma. The 584 Ma peak is known from zircon patterns of orogens that formed during the final amalgamation of NE Gondwana in the late Proterozoic–early Cambrian (e.g., Pinjarra, Kuunga, Paterson-Petermann orogens; Cawood & Buchan, 2007; Martin et al., 2017). The 1,177 Ma peak is typical of orogens and basins of western Australia (Fitzsimons, 2000; Martin et al., 2017), as well as terranes rifted from Australia and amalgamated to Eurasia during the Phanerozoic (Lhasa, West Burma, East Sumatra; Zhang et al., 2018; Zhu, Zhao, Niu, Dilek, & Mo, 2011; Zhu et al., 2011). In contrast, it is expected that sediments derived from Indian Gondwana and related terranes (e.g., Sibusima, south Qiangtang, Tethyan and Greater Himalaya) would yield a major age peak at ca. 950–1,000 Ma (Gehrels et al., 2011; Jonell et al., 2017; Zhang et al., 2018), which is not the case for the Nindam Formation. Therefore, new and existing data support a possible eastward connection of the Dras arc with sources of zircons derived from Australian Gondwana or associated terranes rifted from Australia. This implies that, by 100 Ma, Australian Gondwana-type DZ were transported to the Dras arc from either western Australia or an Australian-derived crustal fragment such as the Lhasa Block. Additional geochemical and isotopic

characterization of igneous and DZs from Ladakh and Tibet would better resolve the nature and timing of Mesozoic connections between the arc-related units exposed along the Indus-Yarlung suture zone.

#### 5.4. Scenarios of the Tectonic Evolution of a Single Dras-Kohistan-Ladakh Arc

Remarkably similar igneous rock and DZ peak ages at ca. 160 Ma of the Dras, Ladakh and Kohistan arcs suggest that these arc remnants were formed at a subduction zone that initiated during the Late Jurassic (Jagoutz et al., 2019; Saktura et al., 2020; Walsh et al., 2020). However, subduction may have been ongoing from at least the Early Jurassic, as suggested by: (a) the Triassic to Early Jurassic DZ of the Nindam Formation; and (b) the Ti/V values ( $\geq 0.15$ ) of the 177 Ma mafic rocks of the Spongtang ophiolite (Corfield et al., 2001), which are compatible with a supra-subduction setting (Shervais, 1982). Whether the Spongtang ophiolite originated at the same convergent margin as the Dras-Kohistan-Ladakh arc remains to be further ascertained (e.g., Parsons et al., 2020).

Late Jurassic intraoceanic arcs may have formed at north-dipping or south-dipping subduction zones. Examples of such configurations are depicted in competing models featuring a Neotethyan intraoceanic arc that is connected along-strike with western Australia (Hall, 2012; Metcalfe, 2021), Lhasa (Parsons et al., 2020; Saktura et al., 2020), or Burma (Licht et al., 2020). Although testing the kinematic feasibility of these models and assumptions is beyond the scope of the present study, we find it unrealistic that a Late Jurassic intraoceanic arc formed over a northward dipping subduction zone along the southern margin of the Lhasa Block. If Lhasa Block's northward motion was accommodated by southward dipping subduction along its northern margin (e.g., Parsons et al., 2020), there is no logical mechanism that can account for subduction initiation along its southern margin. If Lhasa's northward motion was accommodated by northward dipping subduction along its southern margin (e.g., Kapp & DeCelles, 2019), it is unclear how Lhasa could have rifted away from Australia in the absence of a southward dipping subduction beneath its northern margin and how this configuration could have allowed its relatively rapid northward motion (5 cm/yr according to Li et al., 2016). Instead, we assume that northward dipping subduction initiation, forearc extension, and ophiolite generation along the southern margin of the Lhasa Block was only possible after its northward motion had significantly decreased following accretion to Eurasia.

If Lhasa amalgamated with Eurasia after 150 Ma (Latest Jurassic; e.g., Allègre et al., 1984; Dewey et al., 1988; Lai et al., 2019; Li et al., 2016; Li et al., 2019), then 165 Ma supra-subduction ophiolites (e.g., Zedong, Aitchison, McDermid, et al., 2007) that lie south of it must have formed at a separate margin located to the south within the Neotethys. In contrast, a less commonly accepted pre-Late Jurassic accretion of Lhasa to Eurasia would allow episodes of forearc extension and ophiolite generation at its southern margin starting at ca. 165 Ma, which would not preclude the existence of a coeval Neotethyan intraoceanic arc further to the south. Based on the assumptions above, we explore tectonic scenarios in the Ladakh transect and in which a single Dras-Kohistan-Ladakh arc: (a) was laterally continuous with Lhasa above a south-dipping intraoceanic subduction zone south of Eurasia (scenario 1; Figure 8); (b) formed along a north-dipping intraoceanic subduction zone initiated at a mid-ocean ridge located south of Eurasia, with which Lhasa was already amalgamated (scenario 2; Figure 9).

##### 5.4.1. Scenario 1: Dras-Kohistan-Ladakh Arc Formed Above a South-Dipping Subduction Zone

Whether the Karakoram Block and the Kohistan-Ladakh arc were welded together along the Shyok suture zone during the middle Cretaceous (e.g., Borneman et al., 2015; Rolland, 2002) or the Eocene (e.g., Bouilhol et al., 2013; Martin et al., 2020) has direct implications for evaluating the validity of the competing scenarios. A Cretaceous age for the Shyok suture implies that it represents a lateral equivalent of the Cretaceous Bangong suture in Tibet, the logical consequence of which is that these sutures were formed by the closure of an ocean that was bounded to the south by the Dras-Kohistan-Ladakh arc continuous with Lhasa (scenario 1 in Figure 8). A Jurassic southward dipping subduction beneath the Dras-Kohistan-Ladakh arc is similarly argued for Lhasa (Li et al., 2019; Zhu et al., 2009, 2011). The accretion of the Dras-Kohistan-Ladakh arc to Eurasia during the Early Cretaceous (ca. 140 Ma) is compatible with the apparent lull in magmatic activity of those arcs as suggested by zircon ages. A similar age gap (ca. 140–120 Ma) is recorded in the Karakoram Block (Borneman et al., 2015; Heuberger et al., 2007; Searle et al., 1989, 2010). Magmatic activity resumed after reinitiation of northward dipping subduction, which possibly triggered the extension of the accreted arc and the formation of intra- and back-arc basins (Robertson & Collins, 2002; Rolland et al., 2000; Rolland, Picard, Pêcher, Lapierre, et al., 2002). In that scenario, the early Late Cretaceous Saltoro Molasse overlying the Shyok volcanics in the Shyok Suture

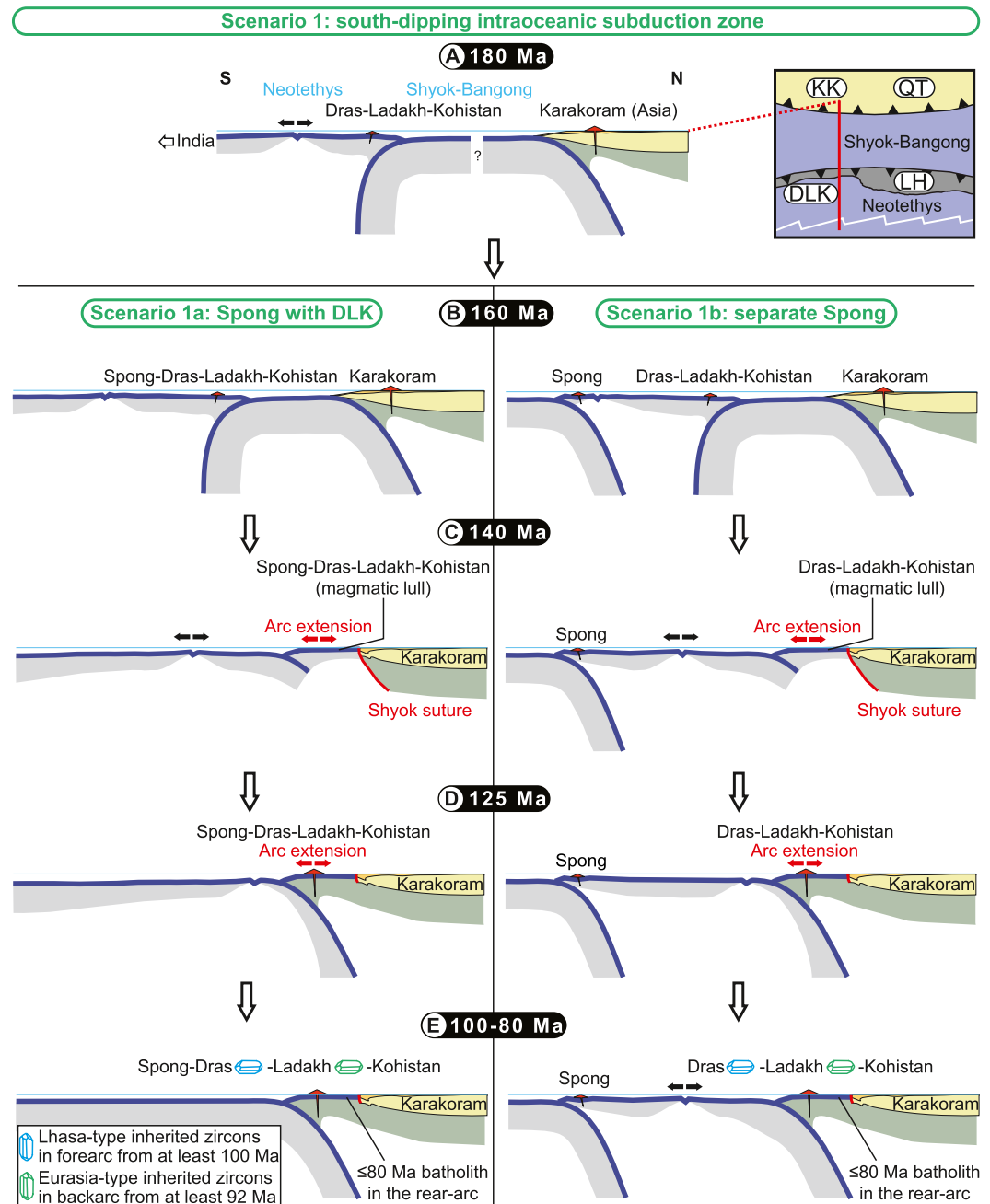


**Figure 8.** Proposed scenario 1 for Mesozoic tectonic evolution of the Dras-Kohistan-Ladakh arc. The Dras-Kohistan-Ladakh arc formed along a southward dipping intraoceanic subduction zone and was laterally continuous with Lhasa toward the east. The Spong arc may or may not be part of the same convergent margin as the Dras-Kohistan-Ladakh arc. See text for discussion. 180 Ma = Early Jurassic; 160 Ma = Late Jurassic; 140 Ma = Early Cretaceous; 125 Ma = Early Cretaceous; 100–80 Ma = Late Cretaceous. KK=Karakoram; QT = Qiangtang; DLK = Dras-Ladakh-Kohistan; LH = Lhasa.

Zone (Figures 3 and 8; Borneman et al., 2015) provides only a minimum age for arc-continent collision and represents sedimentation within a fossil suture zone controlled by back-arc magmatism and tectonics. Finally, scenario 1 requires that the initiation of southward dipping intraoceanic subduction along the Dras-Kohistan-Ladakh arc occurred below a Tethyan oceanic crust located away from the northern margin of India, which allowed the accretion of Upper Permian oceanic intraplate seamounts (Figure 2) to the Spong arc in post-Campanian times (Corfield et al., 1999; Reuber et al., 1987). This is compatible with the absence of DZ inherited from India in the Dras arc, as discussed in Section 5.3.

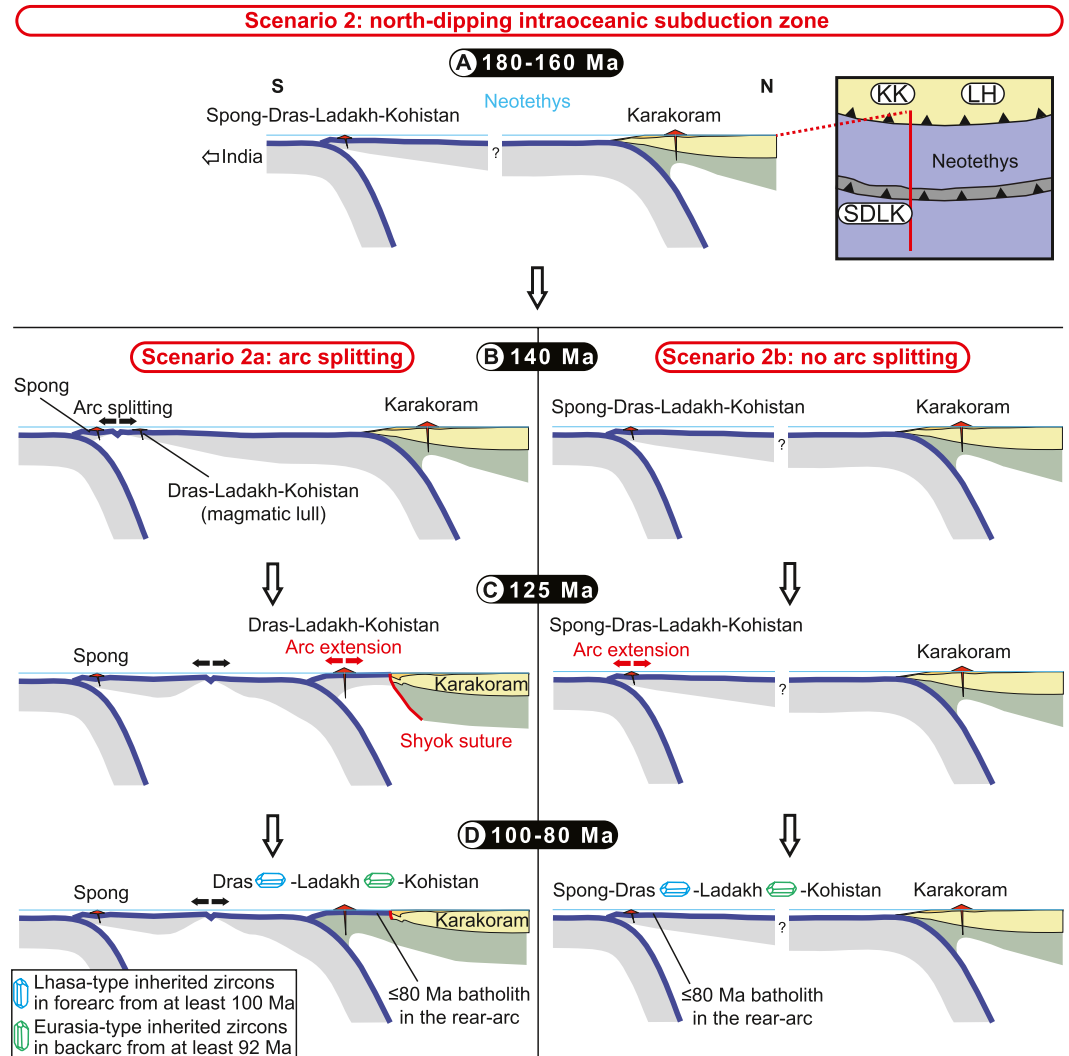


**Figure 9.** Proposed scenario 2 for Mesozoic tectonic evolution of the Dras-Kohistan-Ladakh arc. The Dras-Kohistan-Ladakh formed along a northward dipping intraoceanic subduction zone. Subduction initiation may have occurred as early as the Early Jurassic along a Neotethyan mid-ocean ridge. Pre-Late Jurassic accretion of Lhasa to Eurasia is assumed in scenario 2. See text for discussion. 180–160 Ma = Early to Late Jurassic; 140 Ma = Early Cretaceous; 125 Ma = Early Cretaceous; 100–80 Ma = Late Cretaceous. KK=Karakoram; LH = Lhasa; SDLK=Spong-Dras-Ladakh-Kohistan.

#### 5.4.2. Scenario 2: Dras-Kohistan-Ladakh Arc Formed Above a North-Dipping Subduction Zone

A Cretaceous age of the Shyok suture may be alternatively explained by the accretion of a Dras-Kohistan-Ladakh remnant arc that drifted northward from an intraoceanic arc located within the Neotethys and accreted to the Karakoram Block during the Early Cretaceous (scenario 2a in Figure 9). As discussed above, this implies that Lhasa previously accreted to Eurasia because a northward dipping subduction is needed to allow the remnant arc to move toward Eurasia. This scenario satisfies the observation that Lhasa-type and Eurasia-type DZ were transported to the Dras-Kohistan-Ladakh arc by the middle Cretaceous. However, scenario 2a requires an unlikely correlation between Lhasa and the Karakoram (e.g., Robinson, 2009; Yang et al., 2017) or a reasonable explanation for the absence of an accretion record in the Ladakh transect that is coeval to that of Lhasa in the Tibet transect. In the latter case, a north-south-oriented transform fault within the Tethyan realm could explain a disparate kinematic evolution between the Ladakh and Tibet transects, but it is not supported by regional-scale seismic tomography models, which show seismic mantle anomalies spanning the whole length of the Himalayan orogen (Hafkenscheid et al., 2006; Parsons et al., 2020; van der Voo et al., 1999).

A post-Cretaceous age of the Shyok suture, as assumed in scenario 2b (Figure 9), implies that the Dras-Kohistan-Ladakh arc remained in an intraoceanic arc setting from the Late Jurassic to the Paleocene (e.g., Bouilhol et al., 2013; Jagoutz et al., 2019). Although intraoceanic arcs are known to incorporate inherited zircons from continental sources (Buys et al., 2014; Rojas-Agramonte et al., 2017; Tapster et al., 2014), the apparent absence of connection with a continent or a continental crustal fragment makes scenario 2b the least likely solution to explain the input of Lhasa-type and Eurasia-type zircons in the Dras-Kohistan-Ladakh arc by the middle Cretaceous. A possible mechanism may be arc-parallel transport of old zircons from a source located (a) in Eurasia or (b) along the same subduction zone. In case (a), we speculate that the Dras-Kohistan-Ladakh arc and the Eurasian margin were involved in an arc-arc collision comparable to the one currently taking place between the Izu-Bonin and Honshu arcs (e.g., Draut & Clift, 2013; Underwood & Pickering, 2018). The lower plate position of the colliding intraoceanic arc relative to Eurasia allows continent-derived detritus to be transferred to its forearc basin. In the case of the Izu-Bonin and Honshu collision, forearc-parallel sediment transport is expected over distances of at least 1,000 km because of the downslope between the arc-arc collision zone (ca. 0 m water depth) and the deep-water forearc basin of the colliding intraoceanic arc (ca. 4,000 m water depth). In case (b), a ca. 1,180 Ma DZ peak—typical of the Nindam Formation (Figure 7c; Walsh et al., 2019)—was reported from sedimentary rocks of Western Burma (Sevastjanova et al., 2016; Zhang et al., 2018), which may support a lateral connection between the Dras-Kohistan-Ladakh arc and the Burma Terrane, as recently proposed by Licht et al. (2020) and Westerweel et al. (2020).

Recent paleomagnetic data from the Ladakh arc have been used to constrain a tectonic model similar to scenario 2b (Martin et al., 2020), whereby the Kohistan-Ladakh arc was part of an intraoceanic subduction zone situated at a latitude of  $8.1 \pm 5.6^\circ\text{N}$  at ca. 63 Ma (>500 km south of Eurasia). However, the inferred Paleocene latitude of the Kohistan-Ladakh arc is based on a single paleomagnetic pole. This is regarded as an unreliable approach to infer the allochthony of displaced terranes relative to larger continents (e.g., Eurasia) because, in this case, the proposed single paleomagnetic pole from the Ladakh arc is statistically undistinguishable from the individual poles that compose the paleomagnetic reference frame of continents to which it is compared (Rowley, 2019). Besides not being unambiguously supported by recent paleomagnetic data, scenario 2b suffers from similar flawed assumptions as scenario 2a. It would require: either (a) that Lhasa bypassed the Dras-Kohistan-Ladakh intraoceanic arc during the Late Jurassic before its accretion to Eurasia; or (b) that the Lhasa terrane accreted to Eurasia before the Late Jurassic; or (c) that the Dras-Kohistan-Ladakh arc split from southern Lhasa during the Late Jurassic. As discussed above, these tectonic scenarios are unlikely.

#### 5.4.3. Preferred Tectonic Scenario

An Early Cretaceous accretion of the Dras-Kohistan-Ladakh arc to the Karakoram along the Shyok Suture Zone (scenario 1; Figure 8) and of Lhasa to Qiangtang along the Bangong Suture Zone represents the simplest solution to reconcile the Late Jurassic–Early Cretaceous geology of Ladakh and Tibet. Moreover, scenarios 1a and 1b are the most flexible in terms of accommodating the competing models of India–Eurasia collision (*sensu lato*) at ca. 55 Ma (e.g., Parsons et al., 2020), because they provide both single and double subduction configurations at the time of collision. Finally, the Dras-Kohistan-Ladakh arc may be placed at a northward dipping intraoceanic subduction zone in a variation of scenario 1b, if future geologic and paleomagnetic datasets were to support that tectonic position.

## 6. Conclusion

The adjacent Paleocene Jurutze and Upper Cretaceous Nindam formations in the Zaskar Gorge (Ladakh) present a significant age gap (>20 m.y.) in their DZ maximum depositional ages and dissimilar whole-rock geochemical affinities. This precludes the Jurutze Formation being in a depositional contact with the Nindam Formation in the Zaskar Gorge transect. New and existing data are compatible with the Jurutze and Nindam formations being deposited in distinct parts of the same forearc basin and later tectonically juxtaposed.

The zircon age distributions of the Nindam and Jurutze formations, as well as that of their respective sources (i.e., the Dras and Kohistan-Ladakh arcs), share common peaks at ca. 100 and 160 Ma, which suggests that they were part of the same intraoceanic arc that had been active since at least the Late Jurassic. This is further supported by overlapping U/Yb, Nb/Yb, and Hf compositions of DZ from the Jurutze and Nindam formations. These results

imply that the mélange zones locally separating the Nindam and Jurutze formations may not be interpreted as a suture zone, but rather as intra-arc tectonic contacts.

The Upper Cretaceous Nindam Formation has intermediate major element and depleted trace element whole-rock contents, whereas the Paleocene Jurutze Formation shows intermediate to felsic major element and enriched trace element compositions. This apparent shift in geochemical composition is consistent with the evolution from primitive to mature stages of a single arc, which is also highlighted by decreasing Yb/Gd and increasing Th/U compositions of DZ from the Jurutze and Nindam formations. These results show that a combination of DZ geochronology and geochemistry, and whole-rock geochemistry applied to complex tectonic settings can help correlate sedimentary units of apparently dissimilar age and provenance.

We have explored scenarios for the evolution of a single Dras-Kohistan-Ladakh arc and found that the simplest solution supported by multiple lines of evidence is that of an intraoceanic arc built over a southward dipping subduction zone that accreted to Eurasia during the Early Cretaceous. This solution is the most compatible with the commonly proposed models for Mesozoic evolution of arc-related units exposed in Tibet.

### Conflict of Interest

The authors declare no conflicts of interest relevant to this study.

### Data Availability Statement

All datasets generated during this study have been archived in Zenodo and can be accessed from this link: <https://doi.org/10.5281/zenodo.5705286>.

### Acknowledgments

G.A. thanks the Swiss SNF for funding his postdoctoral fellowship (no. 178098) at the University of Queensland. We thank Jigmet Punchok for assistance in the field. We thank Oliver Jagoutz, Yann Rolland, and the Associate Editor for their useful reviews that helped improve this paper. G.A. thanks Jean-Luc Epard, Bram Vaes, and Douwe van Hinsbergen for interesting discussions on this work.

### References

- Aitchison, J. C., Ali, J. R., & Davis, A. M. (2007). When and where did India and Asia collide? *Journal of Geophysical Research*, *112*, B05423. <https://doi.org/10.1029/2006JB004706>
- Aitchison, J. C., Badengzhu, Davis, A. M., Liu, J., Luo, H., Malpas, J. G., et al. (2000). Remnants of a Cretaceous intra-oceanic subduction system within the Yarlung–Zangbo suture (southern Tibet). *Earth and Planetary Science Letters*, *183*, 231–244. [https://doi.org/10.1016/S0012-821X\(00\)00287-9](https://doi.org/10.1016/S0012-821X(00)00287-9)
- Aitchison, J. C., McDermid, I. R. C., Ali, J. R., Davis, A. M., & Zybrev, S. V. (2007). Shoshonites in southern Tibet record Late Jurassic rifting of a Tethyan intra-oceanic island arc. *The Journal of Geology*, *115*, 197–213. <https://doi.org/10.1086/510642>
- Allégre, C. J., Courtillot, V., Tapponnier, P., Hirn, A., Mattauer, M., Coulon, C., et al. (1984). Structure and evolution of the Himalaya–Tibet orogenic belt. *Nature*, *307*, 17–22. <https://doi.org/10.1038/307017a0>
- Barth, A. P., Tani, K., Meffre, S., Wooden, J. L., Coble, M. A., Arculus, R. J., et al. (2017). Generation of silicic melts in the early Izu-Bonin arc recorded by detrital zircons in proximal arc volcanoclastic rocks from the Philippine Sea. *Geochemistry, Geophysics, Geosystems*, *18*, 3576–3591. <https://doi.org/10.1002/2017GC006948>
- Barth, A. P., Wooden, J. L., Jacobson, C. E., & Economos, R. C. (2013). Detrital zircon as a proxy for tracking the magmatic arc system: The California arc example. *Geology*, *41*, 223–226. <https://doi.org/10.1130/G33619.1>
- Baxter, A. T., Aitchison, J. C., Ali, J. R., Chan, J. S. L., & Chan, G. H. N. (2016). Detrital chrome spinel evidence for a Neotethyan intra-oceanic island arc collision with India in the Paleocene. *Journal of Asian Earth Sciences*, *128*, 90–104. <https://doi.org/10.1016/j.jseas.2016.06.023>
- Baxter, A. T., Aitchison, J. C., & Zybrev, S. V. (2009). Radiolarian age constraints on Mesotethyan ocean evolution, and their implications for development of the Bangong–Nujiang suture, Tibet. *Journal of the Geological Society of London*, *166*, 689–694. <https://doi.org/10.1144/0016-76492008-128>
- Bhat, I. M., Ahmad, T., & Rao, D. S. (2019). The tectonic evolution of the Dras arc complex along the Indus suture zone, western Himalaya: Implications for the Neo-Tethys ocean geodynamics. *Journal of Geodynamics*, *124*, 52–66. <https://doi.org/10.1016/j.jog.2019.01.015>
- Borneman, N. L., Hodges, K. V., Van Soest, M. C., Bohon, W., Wartho, J. A., Cronk, S. S., & Ahmad, T. (2015). Age and structure of the Shyok suture in the Ladakh region of northwestern India: Implications for slip on the Karakoram fault system. *Tectonics*, *34*, 2011–2033. <https://doi.org/10.1002/2015TC003933>
- Bouilhol, P., Jagoutz, O., Hanchar, J. M., & Dudas, F. O. (2013). Dating the India-Eurasia collision through arc magmatic records. *Earth and Planetary Science Letters*, *366*, 163–175. <https://doi.org/10.1016/j.epsl.2013.01.023>
- Buckman, S., Aitchison, J. C., Nutman, A. P., Bennett, V. C., Saktura, W. M., Walsh, J. M. J., et al. (2018). The Spongtang Massif in Ladakh, NW Himalaya: An early cretaceous record of spontaneous, intra-oceanic subduction initiation in the Neotethys. *Gondwana Research*, *63*, 226–249. <https://doi.org/10.1016/j.gr.2018.07.003>
- Buus, J., Spandler, C., Holm, R. J., & Richards, S. W. (2014). Remnants of ancient Australia in Vanuatu: Implications for crustal evolution in island arcs and tectonic development of the southwest Pacific. *Geology*, *42*, 939–942. <https://doi.org/10.1130/G36155.1>
- Cawood, P. A., & Buchan, C. (2007). Linking accretionary orogenesis with supercontinent assembly. *Earth-Science Reviews*, *82*(3–4), 217–256. <https://doi.org/10.1016/j.earscirev.2007.03.003>
- Clift, P. D., Carter, A., Krol, M., & Kirby, E. (2002). *Constraints on India-Eurasia collision in the Arabian Sea region taken from the Indus Group, Ladakh Himalaya, India* (Vol. 195, pp. 97–116). Geological Society of London Special Publications. <https://doi.org/10.1144/GSL.SP.2002.195.01.07>



- Clift, P. D., Degnan, P. J., Hannigan, R., & Blusztajn, J. (2000). Sedimentary and geochemical evolution of the Dras forearc basin, Indus suture, Ladakh Himalaya, India. *The Geological Society of America Bulletin*, *112*, 450–466. [https://doi.org/10.1130/0016-7606\(2000\)112<450:SAGEOT>2.0.CO;2](https://doi.org/10.1130/0016-7606(2000)112<450:SAGEOT>2.0.CO;2)
- Clift, P. D., Hannigan, R., Blusztajn, J., & Draut, A. E. (2002). Geochemical evolution of the Dras–Kohistan arc during collision with Eurasia: Evidence from the Ladakh Himalaya, India. *Island Arc*, *11*, 255–273. <https://doi.org/10.1046/j.1440-1738.2002.00371.x>
- Corfield, R. I., & Searle, M. P. (2000). *Crustal shortening estimates across the North Indian continental margin, Ladakh, NW India* (Vol. 170, pp. 395–410). Geological Society of London Special Publications. <https://doi.org/10.1144/GSL.SP.2000.170.01.21>
- Corfield, R. I., Searle, M. P., & Green, O. R. (1999). Photang thrust sheet: An accretionary complex structurally below the Spontang ophiolite constraining timing and tectonic environment of ophiolite obduction, Ladakh Himalaya, NW India. *Journal of the Geological Society of London*, *156*, 1031–1044. <https://doi.org/10.1144/gsjgs.156.5.1031>
- Corfield, R. I., Searle, M. P., & Pedersen, R. B. (2001). Tectonic setting, origin, and obduction history of the Spontang ophiolite, Ladakh Himalaya, NW India. *The Journal of Geology*, *109*(6), 715–736. <https://doi.org/10.1086/323191>
- Coward, M. P., Windley, B. F., Broughton, R. D., Luff, I. W., Petterson, M. G., Pudsey, C. J., et al. (1986). *Collision tectonics in the NW Himalayas* (Vol. 19, pp. 203–219). Geological Society of London Special Publications. <https://doi.org/10.1144/GSL.SP.1986.019.01.11>
- Dewey, J. F., Shackleton, R. M., Chengfa, C., & Yiyin, S. (1988). The tectonic evolution of the Tibetan Plateau. *Philosophical Transactions of the Royal Society of London*, *327*, 379–413. <https://doi.org/10.1098/rsta.1988.0135>
- Dickinson, W. R., & Gehrels, G. E. (2009). Use of U–Pb ages of detrital zircons to infer maximum depositional ages of strata: A test against a Colorado plateau Mesozoic database. *Earth and Planetary Science Letters*, *288*, 115–125. <https://doi.org/10.1016/j.epsl.2009.09.013>
- Dickinson, W. R., & Suzek, C. A. (1979). Plate tectonics and sandstone compositions. *American Association of Petroleum Geologists' Bulletin*, *63*(12), 2164–2182. <https://doi.org/10.1306/2F9188FB-16CE-11D7-8645000102C1865D>
- Dietrich, V. J., Frank, W., & Honegger, K. (1983). A Jurassic–Cretaceous island arc in the Ladakh–Himalayas. *Journal of Volcanology and Geothermal Research*, *18*(1–4), 405–433. [https://doi.org/10.1016/0377-0273\(83\)90018-5](https://doi.org/10.1016/0377-0273(83)90018-5)
- Draut, A. E., & Clift, P. D. (2006). Sedimentary processes in modern and ancient oceanic arc settings; evidence from the Jurassic Talkeetna Formation of Alaska and the Mariana and Tonga arcs, Western Pacific. *Journal of Sedimentary Research*, *76*(3–4), 493–514. <https://doi.org/10.2110/jsr.2006.044>
- Draut, A. E., & Clift, P. D. (2013). Differential preservation in the geologic record of intraoceanic arc sedimentary and tectonic processes. *Earth-Science Reviews*, *116*, 57–84. <https://doi.org/10.1016/j.earscirev.2012.11.003>
- Dürr, S. B. (1996). Provenance of Xigaze fore-arc basin clastic rocks (cretaceous, South Tibet). *The Geological Society of America Bulletin*, *108*, 6692–7684. [https://doi.org/10.1130/0016-7606\(1996\)108<0669:POXFAB>2.3.CO](https://doi.org/10.1130/0016-7606(1996)108<0669:POXFAB>2.3.CO)
- Fitzsimons, I. C. W. (2000). Grenville-age basement provinces in East Antarctica: Evidence for three separate collisional orogens. *Geology*, *28*(10), 879–882. [https://doi.org/10.1130/0091-7613\(2000\)28<879:GBPIEA>2.0.CO;2](https://doi.org/10.1130/0091-7613(2000)28<879:GBPIEA>2.0.CO;2)
- Fuchs, G. (1979). On the geology of western Ladakh. *Jahrbuch der Geologischen Bundesanstalt Austria*, *122*, 513–540.
- Fuchs, G. (1986). Geology of the Markha–Khurnak region in Ladakh (India). *Jahrbuch der Geologischen Bundesanstalt Austria*, *128*, 403–437.
- Gaetani, M. (1997). The Karakorum block in central Asia, from Ordovician to cretaceous. *Sedimentary Geology*, *109*, 339–359. [https://doi.org/10.1016/S0037-0738\(96\)00068-1](https://doi.org/10.1016/S0037-0738(96)00068-1)
- Gaetani, M., Garzanti, E., Jadoul, F., Nicora, A., Tintori, A., Pasini, M., & Khan, K. S. A. (1990). The north Karakorum side of the Central Asia geopuzzle. *The Geological Society of America Bulletin*, *102*, 54–62. [https://doi.org/10.1130/0016-7606\(1990\)102<0054:TNKSOT>2.3.CO;2](https://doi.org/10.1130/0016-7606(1990)102<0054:TNKSOT>2.3.CO;2)
- Gaetani, M., Jadoul, F., Erba, E., & Garzanti, E. (1993). *Jurassic and Cretaceous orogenic events in the North Karakoram: age constraints from sedimentary rocks* (Vol. 74, pp. 39–52). Geological Society of London Special Publications. <https://doi.org/10.1144/GSL.SP.1993.074.01.04>
- Garzanti, E., Baud, A., & Mascle, G. (1987). Sedimentary record of the northward flight of India and its collision with Eurasia (Ladakh Himalaya, India). *Geodinamica Acta*, *1*, 297–312. <https://doi.org/10.1080/09853111.1987.11105147>
- Garzanti, E., & Van Haver, T. (1988). The Indus clastics: Forearc basin sedimentation in the Ladakh Himalaya (India). *Sedimentary Geology*, *59*, 237–249. [https://doi.org/10.1016/0037-0738\(88\)90078-4](https://doi.org/10.1016/0037-0738(88)90078-4)
- Gazel, E., Hayes, J. L., Ulloa, A., Alfaro, A., Coleman, D. S., & Carr, M. J. (2019). The record of the transition from an oceanic arc to a young continent in the Talamanca Cordillera. *Geochemistry, Geophysics, Geosystems*, *20*, 2733–2752. <https://doi.org/10.1029/2018GC008128>
- Gehrels, G., Kapp, P., DeCelles, P., Pullen, A., Blakey, R., Weislogel, A., et al. (2011). Detrital zircon geochronology of pre-Tertiary strata in the Tibetan–Himalayan orogen. *Tectonics*, *30*, TC5016. <https://doi.org/10.1029/2011TC002868>
- Green, O. R., Searle, M. P., Corfield, R. I., & Corfield, R. M. (2008). Cretaceous–Tertiary carbonate platform evolution and the age of the India–Asia collision along the Ladakh Himalaya (northwest India). *The Journal of Geology*, *116*, 331–353. <https://doi.org/10.1086/588831>
- Grimes, C. B., Wooden, J. L., Cheadle, M. J., & John, B. E. (2015). “Fingerprinting” tectono-magmatic provenance using trace elements in igneous zircon. *Contributions to Mineralogy and Petrology*, *170*, 46. <https://doi.org/10.1007/s00410-015-1199-3>
- Guillot, S., Garzanti, E., Baratoux, D., Marquer, D., Mahéo, G., & de Sigoyer, J. (2003). Reconstructing the total shortening history of the NW Himalaya. *Geochemistry, Geophysics, Geosystems*, *4*(7), 1064. <https://doi.org/10.1029/2002GC000484>
- Hafkenschied, E., Wortel, M. J. R., & Spakman, W. (2006). Subduction history of the Tethyan region derived from seismic tomography and tectonic reconstructions. *Journal of Geophysical Research*, *111*, B08401. <https://doi.org/10.1029/2005JB003791>
- Hall, R. (2012). Late Jurassic–Cenozoic reconstructions of the Indonesian region and the Indian ocean. *Tectonophysics*, *570–571*, 1–41. <https://doi.org/10.1016/j.tecto.2012.04.021>
- Hébert, R., Bezard, R., Guilmette, C., Dostal, J., Wang, C., & Liu, Z. (2012). The Indus–Yarlung Zangbo ophiolites from Nanga Parbat to Namche Barwa syntaxes, southern Tibet: First synthesis of petrology, geochemistry, and geochronology with incidences on geodynamic reconstructions of Neo-Tethys. *Gondwana Research*, *22*(2), 377–397. <https://doi.org/10.1016/j.gr.2011.10.013>
- Henderson, A. L., Najman, Y., Parrish, R., BouDagher-Fadel, M., Barford, D., Garzanti, E., & Ando, S. (2010). Geology of the Cenozoic Indus basin sedimentary rocks: Paleoenvironmental interpretation of sedimentation from the western Himalaya during the early phases of India–Eurasia collision. *Tectonics*, *29*, TC6015. <https://doi.org/10.1029/2009TC002651>
- Henderson, A. L., Najman, Y., Parrish, R., Mark, D. F., & Foster, G. L. (2011). Constraints to the timing of India–Eurasia collision; a re-evaluation of evidence from the Indus basin sedimentary rocks of the Indus–Tsangpo suture zone, Ladakh, India. *Earth-Science Reviews*, *106*, 265–292. <https://doi.org/10.1016/j.earscirev.2011.02.006>
- Heri, A. R., Aitchison, J. C., King, J. A., & Villa, I. M. (2015). Geochronology and isotope geochemistry of Eocene dykes intruding the Ladakh Batholith. *Lithos*, *212–215*, 111–121. <https://doi.org/10.1016/j.lithos.2014.11.001>
- Heuberger, S., Schaltegger, U., Burg, J.-P., Villa, I. M., Frank, M., Dawood, H., et al. (2007). Age and isotopic constraints on magmatism along the Karakoram–Kohistan suture zone, NW Pakistan: Evidence for subduction and continued convergence after India–Asia collision. *Swiss Journal of Geosciences*, *100*, 85–107. <https://doi.org/10.1007/s00015-007-1203-7>

- Honegger, K., Dietrich, V., Frank, W., Gansser, A., Thöni, M., & Trommsdorff, V. (1982). Magmatism and metamorphism in the Ladakh Himalayas (the Indus-Tsangpo suture zone). *Earth and Planetary Science Letters*, *60*(2), 253–292. [https://doi.org/10.1016/0012-821X\(82\)90007-3](https://doi.org/10.1016/0012-821X(82)90007-3)
- Hu, X., Wang, J., BouDagher-Fadel, M., Garzanti, E., & An, W. (2016). New insights into the timing of the India-Asia collision from the Paleogene Quxia and Jialazi formations of the Xigaze forearc basin, South Tibet. *Gondwana Research*, *32*, 76–92. <https://doi.org/10.1016/j.gr.2015.02.007>
- Jagoutz, O., Bouilhol, P., Schaltegger, U., & Müntener, O. (2019). *The isotopic evolution of the Kohistan Ladakh arc from subduction initiation to continent arc collision* (Vol. 483, pp. 165–182). Geological Society of London Special Publication. <https://doi.org/10.1144/SP483.7>
- Jagoutz, O., Royden, L., Holt, A. F., & Becker, T. W. (2015). Anomalously fast convergence of India and Eurasia caused by double subduction. *Nature Geoscience*, *8*, 475. <https://doi.org/10.1038/ngeo2418>
- Ji, W. Q., Wu, F. Y., Chung, S. L., Li, J. X., & Liu, C. Z. (2009). Zircon U–Pb chronology and Hf isotopic constraints on the petrogenesis of Gangdese batholiths, southern Tibet. *Chemical Geology*, *262*, 229–245. <https://doi.org/10.1016/j.chemgeo.2009.01.020>
- Johnston, S. M., & Kylander-Clark, A. R. C. (2021). Outer forearc uplift and exhumation during high-flux magmatism: Evidence from detrital zircon geochemistry of the Nacimiento forearc basin, California, USA. *Geology*, *49*(7), 832–836. <https://doi.org/10.1130/G48627.1>
- Jonell, T. N., Carter, A., Böning, P., Pahnke, K., & Clift, P. D. (2017). Climatic and glacial impact on erosion patterns and sediment provenance in the Himalayan rain shadow, Zaskar River, NW India. *The Geological Society of America Bulletin*, *129*, 820–836. <https://doi.org/10.1130/B31573.1>
- Kapp, P., & DeCelles, P. G. (2019). Mesozoic–Cenozoic geological evolution of the Himalayan-Tibetan orogen and working tectonic hypotheses. *American Journal of Science*, *319*, 159–254. <https://doi.org/10.2475/03.2019.01>
- Kay, S., Jicha, B. R., Citron, G. L., Kay, R. W., Tibbetts, A. K., & Rivera, T. A. (2019). The calc-alkaline Hidden Bay and Kagalaska Plutons and the Construction of the central Aleutian oceanic arc crust. *Journal of Petrology*, *60*(2), 393–439. <https://doi.org/10.1093/ptrology/egy119>
- Khan, S. D., Walker, D. J., Hall, S. A., Burke, K. C., Shah, M. T., & Stockli, L. (2009). Did the Kohistan–Ladakh island arc collide first with India? *The Geological Society of America Bulletin*, *121*, 366–384. <https://doi.org/10.1130/B26348.1>
- Kumar, S., Bora, S., Sharma, U. K., Yi, K., & Kim, N. (2017). Early cretaceous subvolcanic calcalkaline granitoid magmatism in the Nubra-Shyok valley of the Shyok suture zone, Ladakh Himalaya, India: Evidence from geochemistry and U–Pb SHRIMP zircon geochronology. *Lithos*, *277*, 33–50. <https://doi.org/10.1016/j.lithos.2016.11.019>
- Lai, W., Hu, X., Garzanti, E., Xu, Y., Ma, A., & Li, W. (2019). Early Cretaceous sedimentary evolution of the northern Lhasa terrane and the timing of initial Lhasa-Qiangtang collision. *Gondwana Research*, *73*, 136–152. <https://doi.org/10.1016/j.gr.2019.03.016>
- Lakhan, N., Singh, A. K., Singh, B. P., Khogekumar, S., & Oinam, G. (2020a). Evolution of Late Cretaceous to Palaeogene basalt–andesite–dacite–rhyolite volcanic suites along the northern margin of the Ladakh magmatic arc, NW Himalaya, India. *Journal of Earth System Science*, *129*, 108. <https://doi.org/10.1007/s12040-020-1372-6>
- Lakhan, N., Singh, A. K., Singh, B. P., Sen, K., Singh, M. R., Khogekumar, S., et al. (2020b). Zircon U–Pb geochronology, mineral and whole-rock geochemistry of the Khardung volcanics, Ladakh Himalaya, India: Implications for Late Cretaceous to Palaeogene continental arc magmatism. *Geological Journal*, *55*, 3297–3320. <https://doi.org/10.1002/gj.3594>
- Li, S., Yin, C., Guilmette, C., Ding, L., & Zhang, J. (2019). Birth and demise of the Bangong–Nujiang tethyan ocean: A review from the Gerze area of central Tibet. *Earth-Science Reviews*, *208*, 102907. <https://doi.org/10.1016/j.earscirev.2020.103209>
- Li, Z., Ding, L., Lippert, P. C., Song, P., Yue, Y., & van Hinsbergen, D. J. (2016). Paleomagnetic constraints on the Mesozoic drift of the Lhasa terrane (Tibet) from Gondwana to Eurasia. *Geology*, *44*, 727–730. <https://doi.org/10.1130/G38030.1>
- Licht, A., Win, Z., Westerweel, J., Cogné, N., Morley, C. K., Chantraprasert, S., et al. (2020). Magmatic history of central Myanmar and implications for the evolution of the Burma Terrane. *Gondwana Research*, *87*, 303–319. <https://doi.org/10.1016/j.gr.2020.06.016>
- Mahéo, G., Bertrand, H., Guillot, S., Villa, I. M., Keller, F., & Capiiez, P. (2004). The South Ladakh ophiolites (NW Himalaya, India). An intra-oceanic tholeiitic arc origin with implication for the closure of the Neo-Tethys. *Chemical Geology*, *203*(3–4), 273–303. <https://doi.org/10.1016/j.chemgeo.2003.10.007>
- Mahéo, G., Fayoux, X., Guillot, S., Garzanti, E., Capiiez, P., & Mascle, G. (2006). Relicts of an intra-oceanic arc in the Sapi-Shergol mélange zone (Ladakh, NW Himalaya, India): Implications for the closure of the Neo-Tethys ocean. *Journal of Asian Earth Sciences*, *26*, 695–707. <https://doi.org/10.1016/j.jseaes.2005.01.004>
- Martin, C. R., Jagoutz, O., Upadhyay, R., Royden, L. H., Eddy, M. P., Bailey, E., et al. (2020). Paleocene latitude of the Kohistan–Ladakh arc indicates multistage India–Eurasia collision. *Proceedings of the National Academy of Sciences*, *117*(47), 29487–29494. <https://doi.org/10.1073/pnas.2009039117>
- Martin, E. L., Collins, W. J., & Kirkland, C. L. (2017). An Australian source for Pacific-Gondwanan zircons: Implications for the assembly of northeastern Gondwana. *Geology*, *45*(8), 699–702. <https://doi.org/10.1130/G39152.1>
- McDermid, I. R. C., Aitchison, J. C., Davis, A. M., Harrison, T. M., & Grove, M. (2002). The Zedong terrane: A late Jurassic intra-oceanic magmatic arc within the Yarlung–Tsangpo suture zone, southeastern Tibet. *Chemical Geology*, *187*, 267–277. [https://doi.org/10.1016/S0009-2541\(02\)00040-2](https://doi.org/10.1016/S0009-2541(02)00040-2)
- McDonough, W. F., & Sun, S.-S. (1995). The composition of the Earth: Chemical evolution of the mantle. *Chemical Geology*, *120*, 223–253. [https://doi.org/10.1016/0009-2541\(94\)00140-4](https://doi.org/10.1016/0009-2541(94)00140-4)
- Metcalfe, I. (2021). Multiple Tethyan ocean basins and orogenic belts in Asia. *Gondwana Research*, *100*, 87–130. <https://doi.org/10.1016/j.gr.2021.01.012>
- Najman, Y., Jenks, D., Godin, L., Boudagher-Fadel, M., Millar, I., Garzanti, E., et al. (2017). The Tethyan Himalayan detrital record shows that India-Asia terminal collision occurred by 54 Ma in the Western Himalaya. *Earth and Planetary Science Letters*, *459*, 301–310. <https://doi.org/10.1016/j.epsl.2016.11.036>
- Nicora, A., Garzanti, E., & Fois, E. (1987). Evolution of the Tethys Himalaya continental shelf during Maastrichtian to Paleocene (Zaskar, India). *Rivista Italiana di Paleontologia e Stratigrafia*, *92*, 439–496.
- Palin, R. M., Searle, M. P., Waters, D. J., Horstwood, M. S. A., & Parrish, R. R. (2012). Combined thermobarometry and geochronology of peraluminous metapelites from the Karakoram metamorphic complex, North Pakistan; New insight into the tectonothermal evolution of the Baltoro and Hunza Valley regions. *Journal of Metamorphic Geology*, *30*, 793–820. <https://doi.org/10.1111/j.1525-1314.2012.00999.x>
- Parsons, A. J., Hosseini, K., Palin, R. M., & Sigloch, K. (2020). Geological, geophysical and plate kinematic constraints for models of the India-Asia collision and the post-Triassic central Tethys oceans. *Earth-Science Reviews*, *208*, 103084. <https://doi.org/10.1016/j.earscirev.2020.103084>
- Pearce, J. A. (1996). A user's guide to basalt discrimination diagrams St. John's, Newfoundland, Canada, Geological Association of Canada, Short Course Notes. In D. A. Wyman (Ed.), (Vol. 12, pp. 79–113). *Trace Element Geochemistry of Volcanic Rocks: Applications for Massive Sulphide Exploration*.
- Pearce, J. A. (2008). Geochemical fingerprinting of oceanic basalts with applications to ophiolite classification and the search for Archean oceanic crust. *Lithos*, *100*, 14–48. <https://doi.org/10.1016/j.lithos.2007.06.016>

- Phillips, R. J., Parrish, R. R., & Searle, M. P. (2004). Age constraints on ductile deformation and long-term slip rates along the Karakoram fault zone, Ladakh. *Earth and Planetary Science Letters*, 226, 305–319. <https://doi.org/10.1016/j.epsl.2004.07.037>
- Phillips, R. J., Searle, M. P., & Parrish, R. R. (2013). The geochemical and temporal evolution of the continental lithosphere and its relationship to continental-scale faulting: The Karakoram Fault, eastern Karakoram, NW Himalayas. *Geochemistry, Geophysics, Geosystems*, 14, 583–603. <https://doi.org/10.1002/ggge.20061>
- Pudsey, C. J. (1986). The northern suture, Pakistan: Margin of a Cretaceous island arc. *Geological Magazine*, 123(4), 405–423. <https://doi.org/10.1017/S0016756800033501>
- Ravikant, V., Wu, F.-Y., & Ji, W.-Q. (2009). Zircon U–Pb and Hf isotopic constraints on petrogenesis of the Cretaceous–Tertiary granites in eastern Karakoram and Ladakh, India. *Lithos*, 110, 153–166. <https://doi.org/10.1016/j.lithos.2008.12.013>
- Raz, U., & Honegger, K. (1989). Magmatic and tectonic evolution of the Ladakh block from field studies. *Tectonophysics*, 161, 107–118. [https://doi.org/10.1016/0040-1951\(89\)90306-5](https://doi.org/10.1016/0040-1951(89)90306-5)
- Reuber, I. (1989). The Dras arc: Two successive volcanic events on eroded oceanic crust. *Tectonophysics*, 161(1–2), 93–106. [https://doi.org/10.1016/0040-1951\(89\)90305-3](https://doi.org/10.1016/0040-1951(89)90305-3)
- Reuber, I., Colchen, M., & Mevel, C. (1987). The geodynamic evolution of the South-Tethyan margin in Zaskar, NW-Himalaya, as revealed by the Spongtang ophiolitic melanges. *Geodynamica Acta*, 1, 283–296. <https://doi.org/10.1080/09853111.1987.11105146>
- Rex, A. J., Searle, M. P., Tirrul, R., Crawford, M. B., Prior, D. J., Rex, D. C., & Barnicoat, A. (1988). The geochemical and tectonic evolution of the central Karakoram, North Pakistan. *Philosophical Transactions of the Royal Society of London - Series A: Mathematical and Physical Sciences*, 326, 229–255. <https://doi.org/10.1098/rsta.1988.0086>
- Robertson, A. (2000). Formation of mélanges in the Indus suture zone, Ladakh Himalaya by successive subduction-related, collisional and post-collisional processes during late Mesozoic–late Tertiary time. *Geological Society of London Special Publications*, 170(1), 333–374. <https://doi.org/10.1144/GSL.SP.2000.170.01.19>
- Robertson, A. H. F., & Collins, A. S. (2002). Shyok suture zone, N Pakistan: Late Mesozoic–Tertiary evolution of a critical suture separating the oceanic Ladakh arc from the Asian continental margin. *Journal of Asian Earth Sciences*, 20, 309–351. [https://doi.org/10.1016/S1367-9120\(01\)00041-4](https://doi.org/10.1016/S1367-9120(01)00041-4)
- Robertson, A. H. F., & Degen, P. (1994). The Dras arc complex: Lithofacies and reconstruction of a Late Cretaceous oceanic volcanic arc in the Indus suture zone, Ladakh Himalaya. *Sedimentary Geology*, 92, 117–145. [https://doi.org/10.1016/0037-0738\(94\)90057-4](https://doi.org/10.1016/0037-0738(94)90057-4)
- Robertson, A. H. F., Kutterolf, S., Avery, A., Baxter, A. T., Petronotis, K., Acton, G. D., et al. (2018). Depositional setting, provenance, and tectonic–volcanic setting of Eocene–Recent deep-sea sediments of the oceanic Izu–Bonin forearc, northwest Pacific (IODP Expedition 352). *International Geology Review*, 60(15), 1816–1854. <https://doi.org/10.1080/00206814.2017.1393634>
- Robinson, A. C. (2009). Geologic offsets across the northern Karakoram fault: Implications for its role and terrane correlations in the western Himalayan–Tibetan orogen. *Earth and Planetary Science Letters*, 279, 123–130. <https://doi.org/10.1016/j.epsl.2008.12.039>
- Rojas-Agramonte, Y., Williams, I. S., Arculus, R., Kröner, A., García-Casco, A., Lázaro, C., et al. (2017). Ancient xenocrystic zircon in young volcanic rocks of the southern Lesser Antilles island arc. *Lithos*, 290, 228–252. <https://doi.org/10.1016/j.lithos.2017.08.002>
- Rolland, Y. (2002). From intra-oceanic convergence to post-collisional evolution: Example of the India–Asia convergence in NW Himalaya, from Cretaceous to present. *Journal of the Virtual Explorer*, 8, 193–216.
- Rolland, Y., Carrio-Schaffhauser, E., Sheppard, S. M. F., Pêcher, A., & Esclauze, L. (2006). Metamorphic zoning and geodynamic evolution of an inverted crustal section (Karakoram margin, N Pakistan), evidence for two metamorphic events. *International Journal of Earth Sciences*, 95(2), 288–305. <https://doi.org/10.1007/s00531-005-0026-x>
- Rolland, Y., Mahéo, G., Guillot, S., & Pêcher, A. (2001). Tectono-metamorphic evolution of the Karakoram metamorphic complex (Dassu–Askole area, NE Pakistan): Exhumation of mid-crustal HT–MP gneisses in a convergent context. *Journal of Metamorphic Geology*, 19(6), 717–737. <https://doi.org/10.1046/j.0263-4929.2001.00342.x>
- Rolland, Y., Mahéo, G., Pêcher, A., & Villa, I. M. (2009). Syn-kinematic emplacement of the Pangong metamorphic and magmatic complex along the Karakoram fault (N Ladakh). *Journal of Asian Earth Sciences*, 34(1), 10–25. <https://doi.org/10.1016/j.jseaes.2008.03.009>
- Rolland, Y., Pêcher, A., & Picard, C. (2000). Middle Cretaceous back-arc formation and arc evolution along the Asian margin: The Shyok suture zone in northern Ladakh (NW Himalaya). *Tectonophysics*, 325, 145–173. [https://doi.org/10.1016/S0040-1951\(00\)00135-9](https://doi.org/10.1016/S0040-1951(00)00135-9)
- Rolland, Y., Picard, C., Pêcher, A., Carrio, E., Sheppard, S. M., Oddone, M., & Villa, I. M. (2002). Presence and geodynamic significance of Cambro–Ordovician series of SE Karakoram (N Pakistan). *Geodynamica Acta*, 15(1), 1–21. <https://doi.org/10.1080/09853111.2002.10510736>
- Rolland, Y., Picard, C., Pêcher, A., Lapierre, H., Bosch, D., & Keller, F. (2002). The Cretaceous Ladakh arc of NW Himalaya—slab melting and melt–mantle interaction during fast northward drift of Indian Plate. *Chemical Geology*, 182(2/4), 139–178. [https://doi.org/10.1016/S0009-2541\(01\)00286-8](https://doi.org/10.1016/S0009-2541(01)00286-8)
- Rolland, Y., Villa, I. M., Guillot, S., Mahéo, G., & Pêcher, A. (2006). Evidence for pre-Cretaceous history and partial Neogene (19–9 Ma) reequilibration in the Karakoram (NW Himalayan Syntaxis) from 40Ar–39Ar amphibole dating. *Journal of Asian Earth Sciences*, 27(4), 371–391. <https://doi.org/10.1016/j.jseaes.2005.04.008>
- Rowley, D. B. (2019). Comparing paleomagnetic study means with apparent wander paths: A case study and paleomagnetic test of the Greater India versus Greater Indian basin hypotheses. *Tectonics*, 38, 722–740. <https://doi.org/10.1029/2017TC004802>
- Rudnick, R. L., & Gao, S. (2003). Composition of the continental crust. In R. L. Rudnick (Ed.), *Treatise on geochemistry, the crust* (Vol. 3, pp. 1–64). Elsevier.
- Saito, S., & Tani, K. (2017). Transformation of juvenile Izu–Bonin–Mariana oceanic arc into mature continental crust: An example from the Neogene Izu collision zone granitoid plutons, Central Japan. *Lithos*, 277, 228–240. <https://doi.org/10.1016/j.lithos.2016.07.035>
- Saktura, W. M., Buckman, S., Nutman, A. P., & Bennett, V. C. (2020). Late Jurassic Changmar complex from the Shyok ophiolite, NW Himalaya: A prelude to the Ladakh arc. *Geological Magazine*, 158(2), 239–260. <https://doi.org/10.1017/S0016756820000400>
- Schacht, U., Wallmann, K., Kutterolf, S., & Schmidt, M. (2008). Volcanogenic sediment–seawater interactions and the geochemistry of pore waters. *Chemical Geology*, 249, 321–338. <https://doi.org/10.1016/j.chemgeo.2008.01.026>
- Schindlbeck, J. C., Kutterolf, S., Straub, S. M., Andrews, G. D., Wang, K. L., & Mleneck-Vautravers, M. J. (2018). One Million Years tephra record at IODP Sites U1436 and U1437: Insights into explosive volcanism from the Japan and Izu arcs. *Island Arc*, 27(3). <https://doi.org/10.1111/iar.12244>
- Schmitt, A. K., Konrad, K., Andrews, G. D. M., Horie, K., Brown, S. R., Koppers, A. A. P., et al. (2018). 40Ar/39Ar ages and zircon petrochronology for the rear arc of the Izu–Bonin–Marianas intra-oceanic subduction zone. *International Geology Review*, 60(8), 956–976. <https://doi.org/10.1080/00206814.2017.1363675>
- Searle, M. P., & Hacker, B. R. (2019). *Structural and metamorphic evolution of the Karakoram and Pamir following India–Kohistan–Asia collision* (Vol. 483, pp. 555–582). Geological Society of London Special Publications. <https://doi.org/10.1144/SP483.6>

- Searle, M. P., Parrish, R. R., Thow, A. V., Noble, S. R., Phillips, R. J., & Waters, D. J. (2010). Anatomy, age and evolution of a collisional mountain belt: The Baltoro granite batholith and Karakoram metamorphic complex, Pakistani Karakoram. *Journal of the Geological Society of London*, *167*, 183–202. <https://doi.org/10.1144/0016-76492009-043>
- Searle, M. P., Pickering, K. T., & Cooper, D. J. W. (1990). Restoration and evolution of the intermontane Indus molasse basin, Ladakh Himalaya, India. *Tectonophysics*, *174*, 301–314. [https://doi.org/10.1016/0040-1951\(90\)90327-5](https://doi.org/10.1016/0040-1951(90)90327-5)
- Searle, M. P., Rex, A. J., Tirrul, R., Rex, D. C., Barnicoat, A., & Windley, B. F. (1989). *Metamorphic, magmatic, and tectonic evolution of the central Karakoram in the Biafo-Baltoro-Hushe regions of Northern Pakistan* (Vol. 232, pp. 47–74). Geological Society of America Special Paper. <https://doi.org/10.1130/SPE232>
- Sevastjanova, I., Hall, R., Rittner, M., Paw, S. M. T. L., Naing, T. T., Alderton, D. H., & Comfort, G. (2016). Myanmar and Asia united, Australia left behind long ago. *Gondwana Research*, *32*, 24–40. <https://doi.org/10.1016/j.gr.2015.02.001>
- Shellnutt, J. G., Lee, T., Brookfield, M. E., & Chung, S.-L. (2014). Correlation between magmatism of the Ladakh Batholith and plate convergence rates during the India–Eurasia collision. *Gondwana Research*, *26*(3–4), 1051–1059. <https://doi.org/10.1016/j.gr.2013.09.006>
- Shervais, J. W. (1982). Ti–V plots and the petrogenesis of modern and ophiolitic lavas. *Earth and Planetary Science Letters*, *59*(1), 101–118. [https://doi.org/10.1016/0012-821X\(82\)90120-0](https://doi.org/10.1016/0012-821X(82)90120-0)
- Steck, A. (2003). Geology of the NW Indian Himalaya. *Eclogae Geologicae Helveticae*, *96*, 147–196.
- Sutre, E. (1990). *Les formations de la marge nord-néotéthysienne et les mélanges ophiolitiques de la zone de suture de l'Indus en Himalaya du Ladakh, Inde: Stratigraphie, tectonique, évolution géodynamique*. PhD Thesis (p. 295). Poitiers University thesis.
- Tapster, S., Roberts, N. M. W., Petterson, M. G., Saunders, A. D., & Naden, J. (2014). From continent to intraoceanic arc: Zircon xenocrysts record the crustal evolution of the Solomon island arc. *Geology*, *42*(12), 1087–1090. <https://doi.org/10.1130/G36033.1>
- Treloar, P. J., Rex, D. C., Guise, P. G., Coward, M. P., Searle, M. P., Windley, B. F., et al. (1989). K–Ar and Ar–Ar geochronology of the Himalayan collision in NW Pakistan: Constraints on the timing of suturing, deformation, metamorphism and uplift. *Tectonics*, *8*, 881–909. <https://doi.org/10.1029/TC008i004p00881>
- Underwood, M. B., & Pickering, K. T. (2018). *Facies architecture, detrital provenance, and tectonic modulation of sedimentation in the Shikoku Basin: Inputs to the Nankai Trough subduction zone* (Vol. 534, pp. 1–34). Geological Society of America Special Paper. [https://doi.org/10.1130/2018.2534\(01](https://doi.org/10.1130/2018.2534(01)
- Upadhyay, R., Kar, R., & Sinha, A. K. (2004). Palynological evidence for the Palaeocene evolution of the forearc basin, Indus suture zone, Ladakh, India. *Terra Nova*, *16*(4), 216–225. <https://doi.org/10.1111/j.1365-3121.2004.00553.x>
- Van der Voo, R., Spakman, W., & Bijwaard, H. (1999). Tethyan subducted slabs under India. *Earth and Planetary Science Letters*, *171*, 7–20. [https://doi.org/10.1016/S0012-821X\(99\)00131-4](https://doi.org/10.1016/S0012-821X(99)00131-4)
- van Hinsbergen, D. J. J., Lippert, P. C., Li, S., Huang, W., Advokaat, E. L., & Spakman, W. (2018). Reconstructing Greater India: Paleogeographic, kinematic, and geodynamic perspectives. *Tectonophysics*, *760*, 69–94. <https://doi.org/10.1016/j.tecto.2018.04.006>
- Vermeesch, P., Resentini, A., & Garzanti, E. (2016). An R package for statistical provenance analysis. *Sedimentary Geology*, *336*, 14–25. <https://doi.org/10.1016/j.sedgeo.2016.01.009>
- Walsh, J. M. J., Buckman, S., Nutman, A. P., & Zhou, R. (2019). Age and provenance of the Nindam formation, Ladakh, NW Himalaya: Evolution of the intraoceanic Dras arc before collision with India. *Tectonics*, *38*, 3070–3096. <https://doi.org/10.1029/2019TC005494>
- Walsh, J. M. J., Buckman, S., Nutman, A. P., & Zhou, R. (2020). The significance of Upper Jurassic felsic volcanic rocks within the incipient, intraoceanic Dras Arc, Ladakh, NW Himalaya. *Gondwana Research*, *90*, 199–219. <https://doi.org/10.1016/j.gr.2020.11.007>
- Wang, S., Wang, C., Phillips, R. J., Murphy, M. A., & Yue, Y. (2012). Small-scale offset of the Karakoram Fault constrained by LA–ICP–MS U–Pb dating of displaced geological markers. *Earth and Planetary Science Letters*, *337*(338), 156–163. <https://doi.org/10.1016/j.epsl.2012.05.037>
- Weinberg, R. F., Dunlap, W. J., & Whitehouse, M. (2000). *New field, structural and geochronological data from the Shyok and Nubra Valleys, Northern Ladakh: Linking Kohistan to Tibet* (Vol. 170, pp. 253–275). Geological Society of London Special Publications. <https://doi.org/10.1144/GSL.SP.2000.170.01.14>
- Westerweel, J., Licht, A., Cogné, N., Roperch, P., Dupont-Nivet, G., Kay Thi, M., et al. (2020). Burma terrane collision and northward indentation in the eastern Himalayas recorded in the Eocene–Miocene Chindwin basin (Myanmar). *Tectonics*, *39*, e2020TC006413. <https://doi.org/10.1029/2020TC006413>
- White, L. T., Ahmed, T., Ireland, T. R., Lister, G. S., & Forster, M. A. (2011). Deconvolving episodic age spectra from zircons of the Ladakh Batholith, northwest Indian Himalaya. *Chemical Geology*, *289*, 179–196. <https://doi.org/10.1016/j.chemgeo.2011.07.024>
- Wu, F.-Y., Clift, P. D., & Yang, J.-H. (2007). Zircon Hf isotopic constraints on the sources of the Indus molasse, Ladakh Himalaya, India. *Tectonics*, *26*, TC2014. <https://doi.org/10.1029/2006TC002051>
- Yang, Y., Guo, Z., & Luo, Y. (2017). Middle-late Jurassic tectonostratigraphic evolution of central Asia, implications for the collision of the Karakoram–Lhasa block with Asia. *Earth-Science Reviews*, *166*, 83–110. <https://doi.org/10.1016/j.earscirev.2017.01.005>
- Zhang, X. R., Chung, S.-L., Lai, Y.-M., Ghani, A. A., Murtadha, S., Lee, H.-Y., & Hsu, C.-C. (2018). Detrital zircons dismember Sibumasu in east Gondwana. *Journal of Geophysical Research: Solid Earth*, *123*, 6098–6110. <https://doi.org/10.1029/2018JB015780>
- Zhou, R., Aitchison, J. C., Lokho, K., Sobel, E. R., Feng, Y., & Zhao, J.-X. (2020). *Unroofing the Ladakh Batholith: Constraints from autochthonous molasse of the Indus Basin, NW Himalaya* (pp. jgs019–188). Journal of the Geological Society of London. <https://doi.org/10.1144/jgs2019-188>
- Zhu, D. C., Mo, X.-X., Niu, Y., Zhao, Z.-D., Wang, L.-Q., Liu, Y.-S., & Wu, F.-Y. (2009). Geochemical investigation of Early Cretaceous igneous rocks along an east–west traverse throughout the central Lhasa Terrane, Tibet. *Chemical Geology*, *268*, 298–312. <https://doi.org/10.1016/j.chemgeo.2009.09.008>
- Zhu, D. C., Zhao, Z. D., Niu, Y., Dilek, Y., & Mo, X. X. (2011). Lhasa terrane in southern Tibet came from Australia. *Geology*, *39*, 727–730. <https://doi.org/10.1130/G31895.1>
- Zhu, D.-C., Zhao, Z.-D., Niu, Y., Mo, X.-X., Chung, S.-L., Hou, Z.-Q., et al. (2011). The Lhasa terrane: Record of a microcontinent and its histories of drift and growth. *Earth and Planetary Science Letters*, *301*, 241–255. <https://doi.org/10.1016/j.epsl.2010.11.005>

## References From the Supporting Information

- Aitchison, J. C., Xia, X., Baxter, A. T., & Ali, J. R. (2011). Detrital zircon U–Pb ages along the Yarlung–Tsangpo suture zone, Tibet: Implications for oblique convergence and collision between India and Asia. *Gondwana Research*, *20*, 691–709. <https://doi.org/10.1016/j.gr.2011.04.002>
- An, W., Hu, X., Garzanti, E., Boudagher-Fadel, M. K., Wang, J., & Sun, G. (2014). Xigaze forearc basin revisited (South Tibet): Provenance changes and origin of the Yarlung–Tsangpo ophiolite. *The Geological Society of America Bulletin*, *126*, 1595–1613. <https://doi.org/10.1130/B31020.1>

- Black, L. P., Kamo, S. L., Allen, C. M., Davis, D. W., Aleinikoff, J. N., Valley, J. W., et al. (2004). Improved  $^{206}\text{Pb}/^{238}\text{U}$  microprobe geochronology by the monitoring of a trace-element-related matrix effect; SHRIMP, ID-TIMS, ELA-ICP-MS and oxygen isotope documentation for a series of zircon standards. *Chemical Geology*, *205*(1–2), 115–140. <https://doi.org/10.1016/j.chemgeo.2004.01.003>
- Bosch, D., Garrido, C. J., Bruguier, O., Dhuime, B., Bodinier, J.-L., Padrón-Navarta, J. A., & Galland, B. (2011). Building an island-arc crustal section: Time constraints from a LA-ICP-MS zircon study. *Earth and Planetary Science Letters*, *309*, 268–279. <https://doi.org/10.1016/j.epsl.2011.07.016>
- Chen, X. L., Richards, J. P., Liang, H. Y., Zou, Y. Q., Zhang, J., Huang, W. T., et al. (2019). Contrasting arc magma fertilities in the Gangdese belt, southern Tibet: Evidence from geochemical variations of Jurassic volcanic rocks. *Lithos*, *324–325*, 789–802. <https://doi.org/10.1016/j.lithos.2018.12.008>
- Chu, M.-F., Chung, S.-L., Song, B., Liu, D., O'Reilly, S. Y., Pearson, N. J., et al. (2006). Zircon U-Pb and Hf isotope constraints on the Mesozoic tectonics and crustal evolution of southern Tibet. *Geology*, *34*(9), 745–748. <https://doi.org/10.1130/G22725.1>
- Crawford, M. B., & Searle, M. P. (1992). Field relationships and geochemistry of pre-collisional (India-Asia) granitoid magmatism in the central Karakoram, northern Pakistan. *Tectonophysics*, *206*(1–2), 171–192. [https://doi.org/10.1016/0040-1951\(92\)90375-G](https://doi.org/10.1016/0040-1951(92)90375-G)
- Faisal, S., Larson, K. P., King, J., & Cottle, J. M. (2016). Rifting, subduction and collisional records from pluton petrogenesis and geochronology in the Hindu Kush, NW Pakistan. *Gondwana Research*, *35*, 286–304. <https://doi.org/10.1016/j.gr.2015.05.014>
- Fraser, J. E., Searle, M. P., Parrish, R. R., & Noble, S. R. (2001). Chronology of deformation, metamorphism, and magmatism in the southern Karakoram Mountains. *The Geological Society of America Bulletin*, *113*(11), 1443–1455. [https://doi.org/10.1130/0016-7606\(2001\)113<1443:CODMAM>2.0.CO;2](https://doi.org/10.1130/0016-7606(2001)113<1443:CODMAM>2.0.CO;2)
- Guo, L. S., Liu, Y. L., Liu, S. W., Cawood, P. A., Wang, Z. H., & Lui, H. F. (2013). Petrogenesis of early to middle Jurassic granitoid rocks from the Gangdese belt, southern Tibet: Implications for early history of the Neo-Tethys. *Lithos*, *179*, 320–333. <https://doi.org/10.1016/j.lithos.2013.06.011>
- He, S. D., Kapp, P., DeCelles, P. G., Gehrels, G. E., & Heizler, M. (2007). Cretaceous–tertiary geology of the Gangdese arc in the Linzhou area, southern Tibet. *Tectonophysics*, *433*, 15–37. <https://doi.org/10.1016/j.tecto.2007.01.005>
- Heuberger, S. (2004). *The Karakoram-Kohistan suture zone in NW Pakistan–Hindu Kush mountain range. Geological map and explanatory notes*. PhD Thesis (p. 99). Hochschulverlag AG, ETH Zürich.thesis.
- Hu, X., Garzanti, E., Wang, J. G., Huang, W. T., An, W., & Webb, A. (2016). The timing of India-Asia collision onset - Facts, theories, controversies. *Earth-Science Reviews*, *160*, 264–299. <https://doi.org/10.1016/j.earscirev.2016.07.014>
- Jagoutz, O., Burg, J.-P., Hussain, S., Dawood, H., Pettke, T., Iizuka, T., & Maruyama, S. (2009). Construction of the granitoid crust of an island arc part I: Geochronological and geochemical constraints from the plutonic Kohistan (NW Pakistan). *Contributions to Mineralogy and Petrology*, *158*(6), 739–755. <https://doi.org/10.1007/s00410-009-0408-3>
- Jagoutz, O., & Schmidt, M. W. (2012). The formation and bulk composition of modern juvenile continental crust: The Kohistan arc. *Chemical Geology*, *298–299*, 79–96. <https://doi.org/10.1016/j.chemgeo.2011.10.022>
- Ji, W. Q., Wu, F. Y., Chung, S. L., & Liu, C. Z. (2014). The Gangdese magmatic constraints on a latest Cretaceous lithospheric delamination of the Lhasa terrane, southern Tibet. *Lithos*, *210–211*, 168–180. <https://doi.org/10.1016/j.lithos.2014.10.001>
- Jiang, Z., Wang, Q., Wyman, D. A., Shi, X., Yang, J., Ma, L., & Gou, G. (2015). Zircon U–Pb geochronology and geochemistry of Late Cretaceous–early Eocene granodiorites in the southern Gangdese batholith of Tibet: Petrogenesis and implications for geodynamics and Cu  $\pm$  Au  $\pm$  Mo mineralization. *International Geology Review*, *57*(3), 373–392. <https://doi.org/10.1080/00206814.2015.1009503>
- Jiang, Z.-Q., Wang, Q., Wyman, D. A., Li, Z.-X., Yang, J.-H., Shi, X.-B., et al. (2014). Transition from oceanic to continental lithosphere subduction in southern Tibet: Evidence from the Late Cretaceous–early Oligocene (~91–30 Ma) intrusive rocks in the Chanang–Zedong area, southern Gangdese. *Lithos*, *196–197*, 213–231. <https://doi.org/10.1016/j.lithos.2014.03.001>
- Kang, Z. Q., Xu, J. F., Wilde, S. A., Feng, Z. H., Chen, J. L., Wang, B. D., et al. (2014). Geochronology and geochemistry of the Sangri group volcanic rocks, southern Lhasa terrane: Implications for the early subduction history of the Neo-Tethys and Gangdese magmatic arc. *Lithos*, *157–168*. <https://doi.org/10.1016/j.lithos.2014.04.019>
- Lang, X. H., Deng, Y. L., Wang, X. H., Tang, J. X., Yin, Q., Xie, F. W., & Jiang, K. (2020). Geochronology and geochemistry of volcanic rocks of the Bima formation, southern Lhasa subterrane, Tibet: Implications for early Neo-Tethyan subduction. *Gondwana Research*, *80*, 335–349. <https://doi.org/10.1016/j.gr.2019.11.005>
- Leier, A. L., Kapp, P., Gehrels, G. E., & DeCelles, P. G. (2007). Detrital zircon geochronology of Carboniferous–cretaceous strata in the Lhasa terrane, southern Tibet. *Basin Research*, *19*, 361–378. <https://doi.org/10.1111/j.1365-2117.2007.00330.x>
- Li, G., Sandiford, M., Liu, X., Xu, Z., Wei, L., & Li, H. (2014). Provenance of late Triassic sediments in central Lhasa terrane, Tibet and its implication. *Gondwana Research*, *25*, 1680–1689. <https://doi.org/10.1016/j.gr.2013.06.019>
- Ma, L., Wang, Q., Li, Z.-X., Wyman, D. A., Jiang, Z.-Q., Yang, J.-H., et al. (2013b). Early late cretaceous (ca. 93 Ma) norites and hornblendites in the Milin area, eastern Gangdese: Lithosphere–asthenosphere interaction during slab rollback and an insight into early late cretaceous (ca. 100–80 Ma) magmatic “flareup” in southern Lhasa (Tibet). *Lithos*, *17–30*. <https://doi.org/10.1016/j.lithos.2013.03.007>
- Ma, L., Wang, Q., Wyman, D. A., Jiang, Z.-Q., Yang, J.-H., Li, Q.-L., et al. (2013a). Late cretaceous crustal growth in the Gangdese area, southern Tibet: Petrological and Sr–Nd–Hf–O isotopic evidence from Zhengga diorite–gabbro. *Chemical Geology*, *349*(350), 54–70. <https://doi.org/10.1016/j.chemgeo.2013.04.005>
- Meng, Y. K., Dong, H. W., Cong, Y., Xu, Z. Q., & Cao, H. (2016). The early-stage evolution of the Neo-Tethys ocean: Evidence from granitoids in the middle Gangdese batholith, southern Tibet. *Journal of Geodynamics*, *94*(95), 34–49. <https://doi.org/10.1016/j.jog.2016.01.003>
- Meng, Y. K., Santosh, M., Mao, G. Z., Lin, P. J., Liu, J. Q., & Ren, P. (2020). New constraints on the tectono-magmatic evolution of the central Gangdese belt from Late Cretaceous magmatic suite in southern Tibet. *Gondwana Research*, *80*, 123–141. <https://doi.org/10.1016/j.gr.2019.10.014>
- Orme, D. A., Carrapa, B., & Kapp, P. (2015). Sedimentology, provenance and geochronology of the upper cretaceous–lower Eocene western Xigaze forearc basin, southern Tibet. *Basin Research*, *27*, 387–411. <https://doi.org/10.1111/bre.1208>
- Parrish, R. R., & Tirrul, R. (1989). U-Pb age of the Baltoro granite, northwest Himalaya, and implications for monazite U-Pb systematics. *Geology*, *17*(12), 1076–1079. [https://doi.org/10.1130/0091-7613\(1989\)017<1076:UPAOTB>2.3.CO;2](https://doi.org/10.1130/0091-7613(1989)017<1076:UPAOTB>2.3.CO;2)
- Paton, C., Hellstrom, J., Paul, B., Woodhead, J., & Hergt, J. (2011). Iolite: Freeware for the visualisation and processing of mass spectrometric data. *Journal of Analytical Atomic Spectrometry*, *26*(12), 2508–2518. <https://doi.org/10.1039/C1JA10172B>
- Pedersen, R. B., Searle, M. P., & Corfield, R. I. (2001). U-Pb zircon ages from the Spontang ophiolite, Ladakh Himalaya. *Journal of the Geological Society of London*, *158*, 513–520. <https://doi.org/10.1144/jgs.158.3.513>
- Pundir, S., Adlakha, V., Kumar, S., & Singhal, S. (2020). Closure of India–Asia collision margin along the Shyok suture zone in the eastern Karakoram: New geochemical and zircon U–Pb geochronological observations. *Geological Magazine*, *157*, 1451–1472. <https://doi.org/10.1017/S0016756819001547>

- Schärer, U., Copeland, P., Harrison, T., & Searle, M. (1990). Age, cooling history, and origin of post-collisional Leucogranites in the Karakoram batholith: A Multi-system isotope study. *The Journal of Geology*, *98*(2), 233–251. <https://doi.org/10.1086/629395>
- Searle, M. P., Parrish, R. R., Tirrul, R., & Rex, D. C. (1990). Age of crystallization and cooling of the K2 gneiss in the Baltoro Karakoram. *Journal of the Geological Society*, *147*, 603–606. <https://doi.org/10.1144/gsjgs.147.4.0603>
- Singh, S., Kumar, R., Barley, M. E., & Jain, A. K. (2007). SHRIMP U-Pb ages and depth of emplacement of Ladakh Batholith, eastern Ladakh, India. *Journal of Asian Earth Sciences*, *30*, 490–503. <https://doi.org/10.1016/j.jseae.2006.12.003>
- Upadhyay, R., Frisch, W., & Siebel, W. (2008). Tectonic implications of new U–Pb zircon ages of the Ladakh Batholith, Indus suture zone, north-west Himalaya, India. *Terra Nova*, *20*, 309–317. <https://doi.org/10.1111/j.1365-3121.2008.00822.x>
- Upadhyay, R., Sinha, A. K., Chandra, R., & Rai, H. (1999). Tectonic and magmatic evolution of the eastern Karakoram, India. *Geodinamica Acta*, *12*(6), 341–358. <https://doi.org/10.1080/09853111.1999.11105354>
- Weinberg, R. F., & Dunlap, W. J. (2000). Growth and deformation of the Ladakh Batholith, Northwest Himalayas: Implications for timing of continental collision and origin of calc-alkaline batholiths. *The Journal of Geology*, *108*(3), 303–320. <https://doi.org/10.1086/314405>
- Wen, D. R., Chung, S. L., Song, B., Iizuka, Y., Yang, H. J., Ji, J., et al. (2008). Late cretaceous Gangdese intrusions of adakitic geochemical characteristics, SE Tibet: Petrogenesis and tectonic implications. *Lithos*, *105*, 1–11. <https://doi.org/10.1016/j.lithos.2008.02.005>
- Wiedenbeck, M., Alle, P., Corfu, F., Griffin, W., Meier, M., Oberli, F., et al. (1995). Three natural zircon standards for U-Th-Pb, Lu-Hf, trace element and REE analyses. *Geostandards Newsletter*, *19*, 1–23. <https://doi.org/10.1111/j.1751-908X.1995.tb00147.x>
- Wu, F. Y., Ji, W. Q., Liu, C. Z., & Chung, S. L. (2010). Detrital zircon U–Pb and Hf isotopic data from the Xigaze fore-arc basin: Constraints on Transhimalayan magmatic evolution in southern Tibet. *Chemical Geology*, *271*, 13–25. <https://doi.org/10.1016/j.chemgeo.2009.12.007>
- Xie, F., Lang, X., Tang, J., Ma, D., & Zou, B. (2019). Late cretaceous magmatic activity in the southern Lhasa terrane: Insights from the Dazhuqu hornblende gabbro and the Xietongmen granite porphyry. *International Geology Review*, *61*(13), 1642–1665. <https://doi.org/10.1080/00206814.2018.1531273>
- Zhang, Z., Dong, X., Xiang, H., Liou, J. G., & Santosh, M. (2013). Building of the deep Gangdese arc, South Tibet: Paleocene Plutonism and Granulite-Facies metamorphism. *Journal of Petrology*, *54*(12), 2547–2580. <https://doi.org/10.1093/petrology/egt056>
- Zheng, Y. C., Hou, Z. Q., Gong, Y. L., Liang, W., Sun, Q. Z., Zhang, S., et al. (2014). Petrogenesis of Cretaceous adakite-like intrusions of the Gangdese Plutonic Belt, southern Tibet: Implications for mid-ocean ridge subduction and crustal growth. *Lithos*, *190–191*, 240–263. <https://doi.org/10.1016/j.lithos.2013.12.013>